A MODEL FOR THE ATTENUATION OF PEAK GROUND ACCELERATION IN NEW ZEALAND EARTHQUAKES BASED ON SEISMOGRAPH AND ACCELEROGRAPH DATA.

W.J. Cousins[1], J.X. Zhao[1] and N.D. Perrin[1]

1. ABSTRACT

A combination of weak-motion velocity data from seismographs and strong-motion acceleration data from accelerographs has been used to model the attenuation of peak ground acceleration (PGA) in New Zealand earthquakes. The resulting model extends the PGA attenuation model of Zhao, Dowrick and McVerry [30] to include the variability of rock strength, and also describes the unusually high attenuation in the volcanic zone of the North Island of New Zealand.

Strong-rock sites were found to experience lower PGAs than either weak rock or soil sites for magnitudes below M_W 7, and the apparent degree of amplification on going from strong rock to weak rock or soil decreased as the magnitude increased from M_W 5 to M_W 7. At magnitude 7 the PGAs were very similar for all site classes for source distances up to 100 km. When extrapolated to magnitudes beyond the maximum of the data, M_W 7.4, the model predicted that PGAs for strong rock sites were greater than for weak rock or soil sites.

The so-called "whole Taupo Volcanic Zone" was found to provide a good boundary for the zone of high attenuation in the volcanic region of the North Island. The high attenuation was successfully modelled as a simple function of the length of travel path through the zone of high attenuation. Over the effective maximum volcanic path length of about 70 km the extra attenuation resulted in a factor of ten reduction in PGA compared with non-volcanic paths of the same length.

2. INTRODUCTION

A reasonably robust model for the attenuation of PGA in New Zealand has been derived recently by Zhao, Dowrick and McVerry [30]. In it they express PGA as a function of moment magnitude, distance from source, depth, focal mechanism, tectonic type of earthquake and site ground class.

The model is a notable first for New Zealand and reliably covers several aspects of PGA attenuation, but does suffer somewhat from lack of data from genuine rock sites. This is not surprising as the model is based entirely on data from strong-motion accelerographs, the majority of which are located on the type of site of greatest relevance to New Zealand construction, i.e. alluvium. Only 17% of the data used in the study was from "Class A" sites, where "Class A" was defined by Zhao *et al.* as either rock-outcrop (11% of data) or soil layer of up to 3 metres overlying bedrock (6% of data). Importantly only five records, 1% of the New Zealand dataset, were from recorders mounted directly on very strong rock (granite, schist or quartz) and three from recorders directly on moderately strong rock (greywacke or limestone). Twenty records were from recorders on weak rock (weathered greywacke or siltstone). The model of Zhao *et al.* is, therefore, not well suited for providing estimates of PGA at the sites of some important engineering structures, hydro dams for instance.

A second difficulty relates to the distance range of the data used. The New Zealand data, 461 recordings from 51 earthquakes, were recorded at source-to-site distances of 10 to 570 km with the bulk of the data lying in the 30 to 200 km range. Two problems with this data distribution are (i) a lack of control on the shape of the attenuation function both in the very important near-field and at distances above 200 km and (ii) the potential for bias at distances above about 200 km. The lack of shape control arises because of the large scatter in the PGA data, and the potential bias because of the non-triggering of many recorders at the greater distances.

[1] *Institute of Geological & Nuclear Sciences, Lower Hutt, NZ, (Member)*

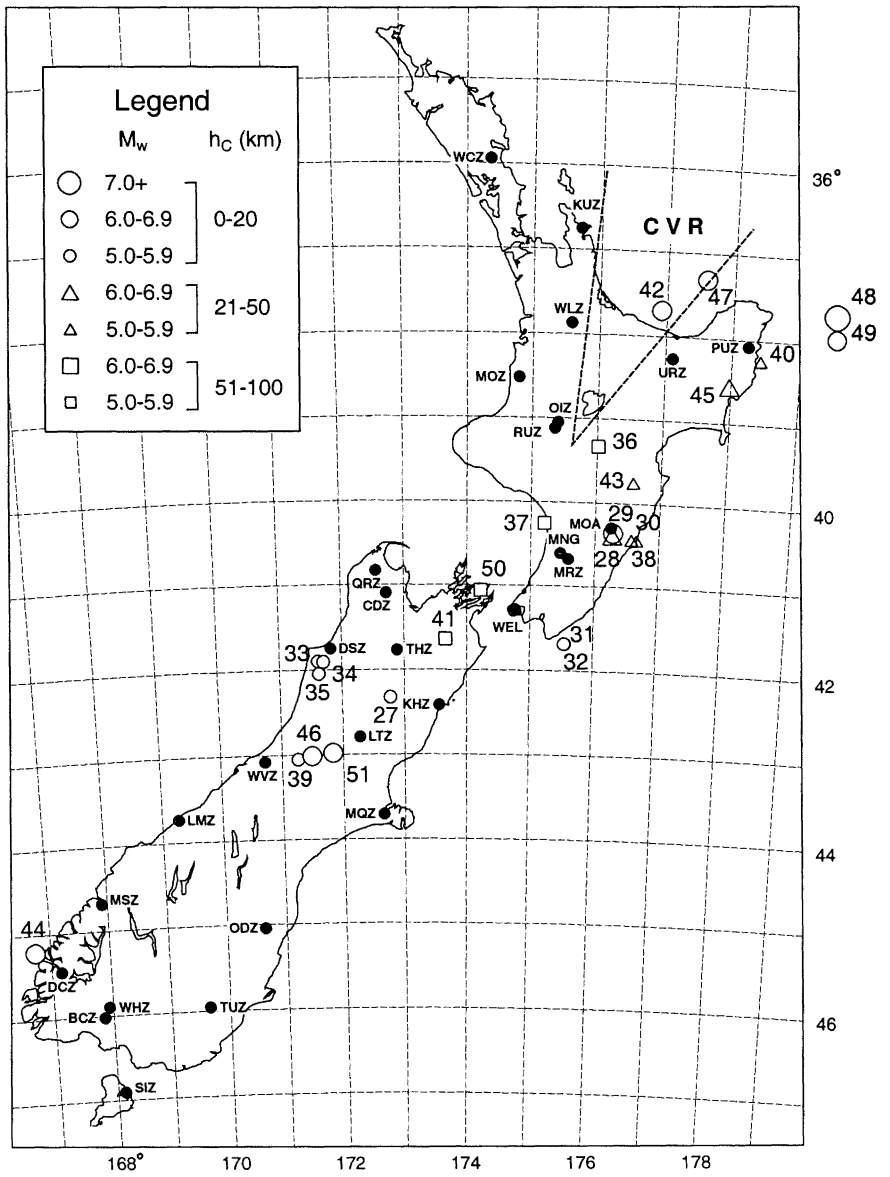

Figure 1: ***Map showing digital 3-component stations in the New Zealand National Seismograph Network along with locations of earthquakes recorded by them and used in the PGA attenuation study. The earthquakes are a subset of those used by Zhao et al. [30]. See Table 2 for further information on the earthquakes.***

Zhao *et al.* overcame the near-field problem by supplementing the New Zealand data with strong-motion recordings from overseas earthquakes, 66 samples from 17 earthquakes, with source-to-site distances of 0.1 to 10 km. The second, far-field, problem however remained unresolved.

In contrast to the kinds of site used in strong-motion recording, those selected for the National Seismograph Network (NSN) (Figure 1) are nearly all on rock. In most cases the underlying rock is classified as either very strong (e.g. quartzite) or moderately strong (e.g. Greywacke) and in only a few cases as weak (e.g. siltstone). Hence it is an attractive proposition to use seismic recordings from the NSN to provide the missing rock data for PGA attenuation modelling.

Two other advantages of the NSN data arise from the relatively very high sensitivity of the seismographs. Firstly, the maximum source distance can be increased over that set for the Zhao *et al.* study, from 500 km to more than 1000 km, and secondly, recordings can be expected from all operational NSN stations for all significant earthquakes on or near the New Zealand landmass, which minimises any bias in the data that might be caused by non-triggered instruments. There is, however, a downside to the high sensitivity of the NSN stations in that they are easily overloaded and so the minimum source distance is about 50 to 150 km, depending of the magnitude of a given event. There is then a potential undesirable feature of largely non-overlapping data sets when the accelerograph and seismograph data sets are combined.

The instruments of the New Zealand accelerograph and seismograph networks are very different from each other and have quite different monitoring purposes. The accelerographs (strong-motion) measure acceleration and are intended to

provide information on ground shaking that is strong enough to be damaging to buildings and other structures. Hence they are typically located on alluvial sites in or close to towns and urban areas. Many are located in structures (buildings, hydro dams and bridges) so as to measure the responses of the structures to strong ground shaking. The seismographs (weak-motion) usually measure ground velocity and are intended to provide information on earthquakes. They are much more sensitive than strong-motion recorders and are usually sited on rock well away from urban areas and other sources of seismic noise. Hence there is a need to show that acceleration waveforms derived from the two types of instrument are sufficiently similar that peak ground accelerations derived from them can be combined for attenuation modelling. This is done in Section 3 where the instruments are described in more detail than above and the results of a period of simultaneous monitoring at one site are given.

Zhao *et al.* demonstrated that their model was suitable for all of New Zealand apart from the Central Volcanic Region of the North Island, labelled CVR in Figure 1. They noted that there was an anomalously high level of attenuation in the CVR but did not have sufficient data to attempt to model it. Recently the high rate of attenuation has been confirmed and modelled for Modified Mercalli Intensity by Dowrick and Rhoades [11].

One reason for a lack of strong-motion data from the CVR is that the high attenuation there means that only rarely have amplitudes been sufficient to trigger strong-motion recorders located within the CVR, and only very rarely are there strong-motion recordings for which the path is completely through the CVR. In this regard the high sensitivity of the seismographs means that there is a significant number of weak-motion records for which the direct path is either partially or completely through the CVR.

3. COMPARISON OF ACCELEROGRAPH AND SEISMOGRAPH DATA

3.1 Instrument characteristics

3.1.1 Accelerograph (and acceleroscope) recording

Strong-motion recording in New Zealand is carried out with a variety of types of acceleroscope and accelerograph [7]. The network operated by GNS (Institute of Geological & Nuclear Sciences) comprises 165 film-recording accelerographs, 77 digital accelerographs, and 65 scratch-plate acceleroscopes.

The film-recording accelerograph records accelerations in three orthogonal directions as high-definition traces on unperforated 35 mm film [14]. Accelerations are measured with damped pendula which deflect light beams in proportion to the accelerations. The accelerograph is normally in stand-by mode and is switched on by a vertically sensing geophone when the acceleration reaches approximately 0.01g. The dynamic properties of the pendulum accelerometers are natural frequency 30 Hz and critical damping ratio 0.6, giving an acceleration sensitivity that is essentially constant from 0 to 25 Hz.

Three types of digital recorder are used, Terra Technology Corporation types DCA-333R (12-bit resolution), IDS3602 (16-bit), and GSR-12/FB (12-bit). All are fitted with triaxial servo accelerometers of 2g full-scale capacity, have pre-event memory of at least 4 seconds, and real-time clocks. The sampling interval is 0.01s for the DCA and 0.004 s for the IDS and GSR instruments. The dynamic properties of the servo accelerometers are critical damping ratio 0.7 and frequency range 0 to at least 30 Hz.

The acceleroscope is a two-component "scratch-plate" type. It gives a trace of the acceleration in the horizontal plane, allowing the amplitude and direction of the maximum horizontal acceleration to be determined. Acceleration is sensed with a damped pendulum and is recorded as a line scribed in a thin layer of smoke-blackened wax on a glass disk of 13 mm diameter. The scriber is a specially sharpened sewing needle. Peak accelerations can be read from the output scratch pattern, but no time information is available.

3.1.2 Seismograph recording

Digital seismograph recording in New Zealand is based on the triaxial Mark Products L4C geophone (velocity transducer) and the locally manufactured EARSS digital data recorder [12]. The EARSS incorporates a gain-ranging amplifier, anti-alias filtering, A/D conversion and sampling at either 0.01 or 0.02 seconds. The nominal natural frequency of the transducer is 1 Hz and the critical damping ratio 0.7, giving a velocity sensitivity that is essentially constant from 1.5 Hz to about 20 Hz [17].

One site, WEL (Figure 1), is monitored with a Kinemetrics triaxial force balance accelerometer (FBA) in place of the velocity transducer. Characteristics of the FBA are full scale 0.5g, output 5 volts/g, natural frequency 50 Hz and damping 0.7 of critical.

3.2 Digitisation and computer processing

Several methods have been used for the digitisation of the film accelerograms over the last thirty years of monitoring. The earliest films were digitised point-by-point by hand using a travelling microscope, a method that was (thankfully) superseded by a commercial hand digitizer (Hewlett-Packard model 9874A), which in turn was superseded by an automatic curve follower based on a reflectance sensor attached to the pen carriage of a digital plotter. Currently film accelerograms are scanned with a Hewlett-Packard SCANJET scanner at a resolution of 600 d.p.i., and the resulting TIFF files are converted to vector format using SMA SCANVIEW software from Kinemetrics/Systems.

Routine computer processing of accelerograms consists of (i) conversion to standard units of acceleration using static sensitivity values and (film accelerograms only) correction for cross-axis effects [25], and (ii) correction for the dynamic frequency response of the accelerometer pendulums (film recorders only), and band-pass filtering. The dynamic corrections and filtering are carried out in the frequency domain [15]. Aliasing is prevented by low-pass filtering at 25 Hz, and low-frequency noise is removed by high-pass filtering at,

typically, 0.15 to 0.5 Hz, with a transition bandwidth of 0.15 to 0.2 Hz and a sinusoidal transition function. The high-pass filter frequency is selected visually, on a record-by-record basis, by comparing the Fourier amplitude spectrum calculated from the accelerogram in question with an appropriate noise spectrum [9]. The final sampling interval is 0.02 s.

Seismogram processing for the PGA attenuation study commenced with inspection of the velocity traces for clipping and other abnormalities. Traces that were free from abnormalities were then processed in the frequency domain as follows: differentiation to give acceleration time histories, dynamic instrument correction to extend the low-frequency limit to about 0.5 Hz, and high-pass filtering. A high-pass filter frequency of 0.5 Hz was found necessary for suppression of low-frequency noise. Low-pass filtering was not needed at this stage of processing because an anti-alias filter is built-in to the EARSS recorder.

Records from the FBA were treated similarly with the exception that no differentiation step was required.

Several of the seismograph velocity records were clipped, and because the clipped records tended to be the most valuable near-source ones in the seismograph dataset some effort was made to retain them. Fortunately, only peak accelerations were required for the attenuation modelling, and because the peaks in the derived acceleration records tended to occur close to the zero points of the original velocity records, clipping of the velocity records *per se* was not necessarily a problem. The following procedure was used to guide the retention or rejection of each clipped record.

Firstly, the time of the peak acceleration was located and a few second segment of the velocity trace surrounding that time was plotted for inspection and so that the dominant frequency could be estimated. Then the most likely cause of the clipping was determined, the possibilities considered being either the mechanical capabilities of the L4C transducer (±5 mm maximum displacement from rest position, 0.5 to 20 Hz frequency range) or the voltage input limit at the A/D converter of the EARSS system.

In all cases the cause of the clipping seemed to be the limit set by the voltage range of the A/D converter. The dominant frequencies in the clipped records at the times of the peak accelerations were in the range 2 to 5 Hz, and at these frequencies the amplitudes of the recorded motions appeared to be well below the transducer's displacement limit.

For a few records the velocities and frequencies were such that the PGAs were clipped (i.e. adjacent velocity samples had +max. and -max. values). Those records were discarded. For about 25% of the clipped records the degree of clipping was minor. Those were processed in the frequency domain in the same manner as unclipped records. For the remaining records where the degree of clipping was moderate to severe, but accelerations did not appear to be clipped, the frequency domain processing did not seem to cope well with the truncated waveforms and so a simple $\Delta v/\Delta t$ method of differentiation was used instead.

3.3 Comparisons

For a period of 4 months from late November 1994, an EARSS:L4C system and an IDS digital accelerograph were operated together in a concrete bunker at GNS's former Seismological Observatory at Kelburn, Wellington. For operational reasons the instruments had to be located in separate rooms of the bunker, but were less than 2 metres apart. Also in the bunker was the NSN site WEL which was equipped with a force balance accelerometer (FBA) and an EARSS recorder.

During the 4 month period six events were recorded simultaneously on the L4C and IDS systems. All 12 records were processed and the results compared visually using overlays of time history plots and Fourier amplitude spectra. The results were as follows:

- N90E component: excellent agreement for acceleration time-histories, Fourier amplitude spectra (especially over the frequency range 0.5 to 10 Hz), and PGAs. Discrepancies between the waveforms and peaks were at most minor, and often were clearly a result of the sampling process.

- N00E component: there were some discrepancies between both time histories and Fourier spectra, but the correspondence appeared good enough for the purpose of deriving PGAs.

- UP component: although the two instruments were clearly trying to reproduce the same waveforms there were some significant differences between the traces for most of the records. The EARSS:L4C system appeared to have a significantly higher response than the IDS over the frequency range 12 to 15 Hz, and a lower response from 15 to 20 Hz. PGAs from the EARSS:L4C system were consistently higher than those from the IDS accelerograph.

PGAs derived from the two systems are compared in Table 1. Overall the results indicate that horizontal component PGAs derived from the EARSS:L4C system can be used with considerable reliability to supplement data derived from the strong-motion accelerographs. In fact, in some respects the similarity between the waveforms could be considered remarkable given the great differences between the two systems.

Three of the events, 5-2-95, 10-2-95 and 22-3-95, were also recorded by the EARSS:FBA system. Comparisons of PGAs showed (i) in the horizontal directions the EARSS:FBA system gave readings that were on average about 10% smaller than those from the other two systems, and (ii) in the vertical direction the EARSS:FBA system gave PGAs that were on average 5% larger than those from the EARSS:L4C system.

In summary, the above results suggest that horizontal PGAs derived from an EARSS:L4C system are quite adequate for the purpose of PGA attenuation modelling.

Table 1: Comparison of peak ground accelerations derived from earthquake motions recorded simultaneously on an EARSS:L4C seismograph system and an IDS accelerograph. The two instruments were located approximately 2 m apart in a concrete bunker at the former Seismological Observatory site in Kelburn.

Event date	magnitude M_L	PGA (g)	PGA ratio, EARSS:L4C/IDS			
			N90E	N00E	horiz	UP
15-12-94	5.2	0.009	1.00	1.02	0.99	1.08
20-12-94	4.5	0.002	0.99	0.91	1.01	1.29
6-1-95	5.0	0.004	0.88	1.15	0.98	1.68
5-2-95	6.8	0.003	1.00	0.87	0.99	1.19
10-2-95	6.2	0.001	1.00	0.91	0.94	1.01
22-3-95	6.5	0.077	0.99	0.97	0.99	1.16
Mean ratio (± sd)			0.98±0.05	0.97±0.10	0.98±0.02	1.24±0.24

4. NEW ZEALAND EARTHQUAKES STUDIED

The earthquakes considered in the seismogram part of our study were a subset of those used by Zhao *et al.* for their strong-motion PGA attenuation study [30], i.e. the 25 events, post 1989, for which three-component digital seismogram data were available (Table 2). In common with the Zhao *et al.* approach M_W was used as the measure of magnitude, and "depth to the centroid of rupture" as the measure of depth. The locations of the earthquakes are shown in Figure 1 and the distribution of depths and magnitudes in Figure 2(a, b). We also made use of the full Zhao *et al.* accelerogram dataset including their overseas data.

5. SEISMOGRAM DATA SET

A total of 328 weak-motion records were available from National Network stations, giving a seismograph PGA dataset potentially 70% as large as the Zhao *et al.* accelerograph dataset. For the period 1990 to 1995 inclusive the two datasets were almost equal in size.

In four of the records the accelerations were clipped and the records were therefore discarded. In a further 28 cases the velocities of at least one component were clipped, but the accelerations did not appear to have been artificially limited, and so the PGA values were retained in the dataset.

A further 50 seismograph records were obtained from a network that was deployed temporarily in the north-eastern part of the CVR, the Taupo Volcanic Zone (TVZ), during the period January 1995 to May 1995. Three major events were recorded by the temporary network, two centred offshore of East Cape on the 5th and 10th of February 1995, and one near Wellington on the 22nd of March 1995 (events 48, 49 and 50 of Table 2).

PGAs in the seismograph dataset ranged from 2 x 10^{-6}g to 0.076g, and source distances from 30 to 1320 km (Figure 2(b)).

Not all of the seismograph records were used directly in developing the attenuation model. In order to minimise the risk of bias all records at distances of more than 400 km from source were excluded from the modelling process. The reasons for this are discussed more fully later. Such data were however included in single-event attenuation plots as part of the process of evaluating the resultant models. The final modelling dataset contained 676 values. Of these 72% were from accelerographs and 28% from seismographs, with 40% of the total being from rock sites and 60% from soil sites.

6. SITE CLASSIFICATIONS

New Zealand's strong-motion accelerograph sites have been classified into three site classes, A, B and C according to criteria given in the New Zealand loadings code [23], as follows;

- A — rock or very stiff soil sites with natural periods less than 0.25 s,
- B — intermediate sites, and
- C — flexible or deep sites with natural periods greater than 0.6 s.

The "rock" sites, Class A, can be further subdivided into classifications R, T, L, and V [8, 30], defined as:

- AR — **R**ock outcrop

AT Topographic effects expected,
AV Very thin soil layer (≤ 3 m) overlying bedrock, and
AL thin soil Layer (> 3 m) overlying bedrock.

Table 2: List of earthquakes yielding digital seismogram data for the PGA attenuation study.

No.[1]	Date yyyy mm dd	UT hh:mm	Epicentre °S °E	M_W	Centroid Depth (km)	Tect. Type[2]	Predom Source Mech.[3]
27	1990 02 10	03:27	42.32 172.74	5.93	8	C	S
28	1990 02 19	05:34	40.38 176.22	6.23	27	S	N
29	1990 05 13	04:23	40.35 176.23	6.37	13	C	R
30	1990 08 15	15:54	40.32 176.44	5.17	28	S	N
31	1990 10 04	23:48	41.60 175.41	5.57	15	I	R
32	1990 10 06	02:41	41.60 175.41	5.46	15	I	R
33	1991 01 28	12:58	41.89 171.58	5.79	10	C	R
34	1991 01 28	18:00	41.90 171.67	5.93	11	C	R
35	1991 02 15	10:48	42.04 171.59	5.42	9	C	R
36	1991 07 12	04:42	39.31 175.97	5.30	69	S	S
37	1991 09 08	13:50	40.25 175.17	5.61	94	S	R
38	1992 03 02	09:05	40.31 176.48	5.54	26	S	N
39	1992 03 30	07:02	43.05 171.23	5.50	5	C	R
40	1992 05 16	17:57	38.23 178.37	5.76	22	I	R
41	1992 05 27	22:30	41.63 173.62	5.88	67	S	S
42	1992 06 21	17:43	37.67 176.86	6.25	4	C	N
43	1993 04 11	06:59	39.74 176.52	5.63	24	I	R
44	1993 08 10	00:51	45.21 166.71	6.81	22	I	R
45	1993 08 10	09:46	38.52 177.87	6.19	39	S	S
46	1994 06 18	03:25	43.01 171.46	6.81	4	C	R
47	1994 12 15	11:20	37.27 177.53	6.31	12	C	S
48	1995 02 05	22:51	37.65 179.49	7.09	10	C	N
49	1995 02 10	01:45	37.92 179.51	6.49	10	C	N
50	1995 03 22	19:43	41.05 174.18	5.83	90	S	S
51	1995 11 24	06:19	42.98 171.80	6.24	5	C	S

Notes:
1. *Event reference number as in Zhao et al. [30]*
2. *Tectonic Type: C = crustal, I = interface, S = slab*
3. *Predominant Source Mechanism: N = normal, R = reverse, S = strike-slip. (A mixed event, say partly R and partly S, is defined as predominantly R if the ratio of the components R/S is ≥ 1.0)*

Zhao *et al.* [30] found in their PGA study that only two categories could be separated with statistical significance, "rock" (combining subdivisions AR, AT and AV) and "soil" (combining subdivisions AL, B and C). Postulated "deep" and "soft" subdivisions of classes B and C were found not to be significant, and the scarcity of data from rock sites prevented any more detailed investigation of the "rock" subdivisions.

For the present study the "rock" category was initially subdivided into "very strong", "moderately strong" or "weak" according to the geological nature of the underlying materials. The types of rock assigned to each subdivision were based largely on the classes described by Borcherdt [3], as listed below in Table 3. A departure from the Borcherdt classification was that the "weak rock" category as defined here consisted of just the weak or soft types of bedrock and did not include any gravelly soils. The subdivisions also correspond essentially to the NEHRP (1994) categories A (hard rock), B (rock) and C (soft rock) [22].

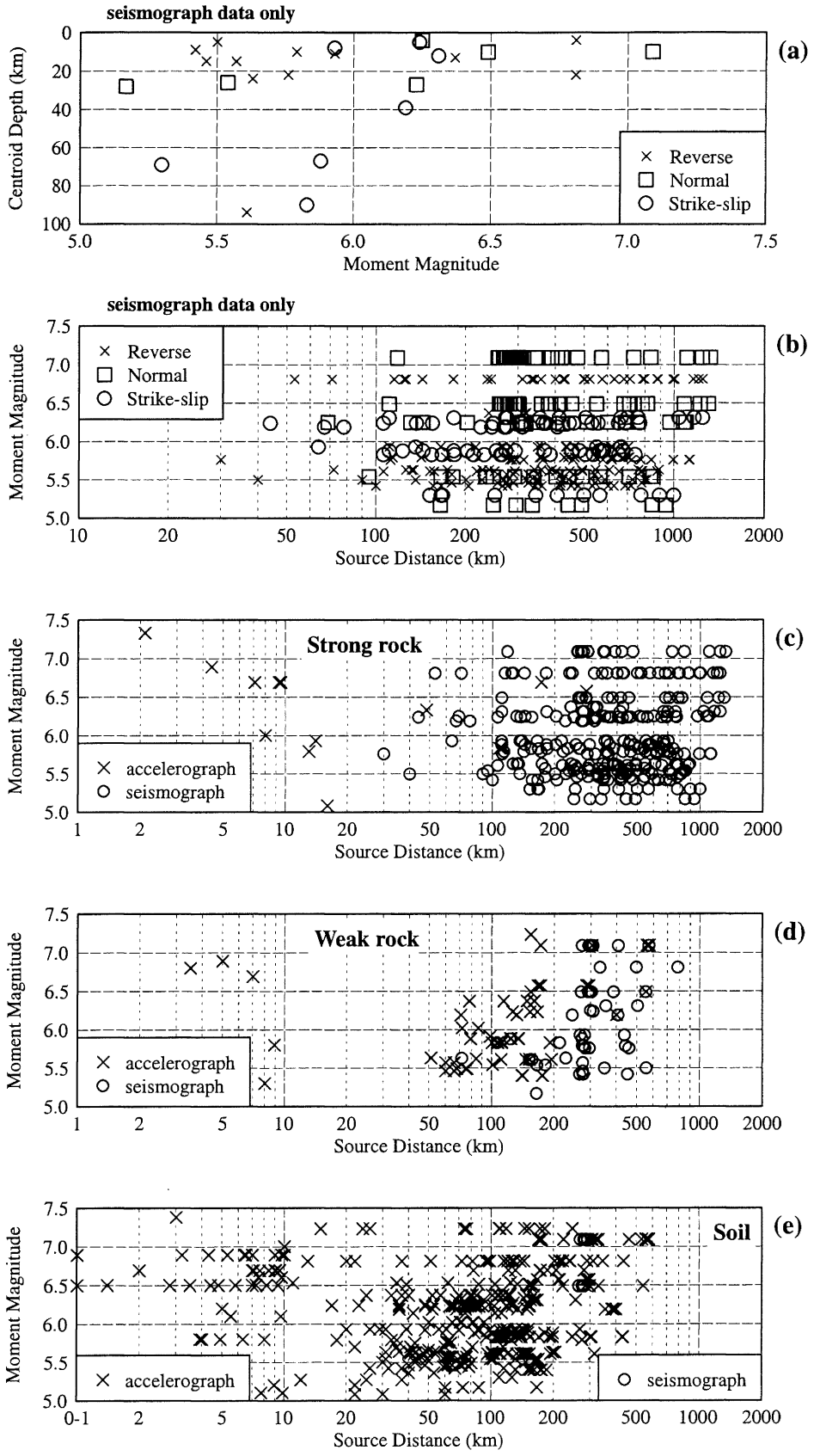

Figure 2: ***(a-b) Centroid depth h_c, focal mechanism and moment magnitude M_w for the New Zealand earthquakes yielding digital seismograph data for the PGA attenuation study.***
(c-e) Moment magnitude, site category and type of record for the combined seismograph and accelerograph data sets. Most of the data points for source distances smaller than 10 km are from overseas earthquakes. Data at source distances greater than 400 km were excluded from the modelling process, but were displayed in verification plots.

Table 3: Rock strength categories as used in the PGA attenuation study. The mean shear-wave velocities are those associated with the Borcherdt classes.

Category	Very Strong	Moderately Strong	Weak
Borcherdt class	**SC-Ia**	**SC-Ib**	**SC-II**
Mean shear wave velocity (m/s)	> 1400	700 – 1400	375 – 700
General Description	Indurated rocks with very widely spaced fractures	Granites, igneous rocks, conglomerates, sandstones and shales with close to widely spaced fractures	soft igneous sedimentary rocks, sandstones and shales
New Zealand Rock types Assigned to Each category	Quartzite Gneiss Granite (in part) Basalt (in part)	Sandstone (calcareous cemented Tertiary) Greywacke (unweathered to slightly weathered) Limestone (fine grained) Schist Marble (in part) Granite (in part) Rhyolite/Andesite/Dacite Ignimbrite (welded) Basalt (in part)	Conglomerate Breccia Sandstone (Tertiary only) Mudstone/siltstone/ Claystone ("papa") Limestone (soft, friable shelly) Tephra Coal/Lignite Crush zone Serpentine Ignimbrite (unwelded) Greywacke (moderately to completely weathered)

Based on the above classification scheme only three of the accelerograph "rock" recording sites can be described as "very strong" rock sites and a further three as "moderately strong" (Appendix 1). Most fall into the categories "weak" rock and bedrock overlain by a thin layer of up to 3 m of soil.

Brief geological descriptions of the seismograph recording sites also are given in Appendix 1. For the National Seismograph Network eight sites are underlain directly by "very strong" rock, sixteen (the majority) by "moderately strong" rock and four by "weak" rock.

For the temporary array in the TVZ, seven sites were classified as "moderately strong" rock, six as "weak" rock, and six as "soil". However there are uncertainties about some of the TVZ site descriptions. For some it is not clear whether a "rock outcrop" is part of a substantial layer of rock or whether it is just the top of a large boulder. Site TEAV is one such site where the surrounding material is described as Taupo pumice alluvium but the instrument was apparently located on ignimbrite. For at least one other, PKUV, the site appeared to be at the edge of a substantial body of rock, but the wide range of possible shapes for the subterranean part of the body of rock meant that its seismic response class was very uncertain.

7. DEVELOPMENT OF THE ATTENUATION MODEL

7.1 Development path

In principal many factors can be isolated and built-in to an attenuation model. Zhao *et al.* [30] modelled the effects of magnitude, distance, source depth, focal mechanism, tectonic type of the earthquake and site ground class. They discussed the high attenuation in the CVR but, because of a lack of suitable data, did not include the CVR effect in their model. Neither did they attempt to model directional effects, once again because a very much larger data set than theirs would have been required for satisfactory results.

The original aim of the seismogram study was to generate additional "rock" class data to supplement that available to the strong-motion PGA model of Zhao *et al.* As modelling progressed, however, it became very clear that the seismograph rock sites were different from the accelerograph rock sites. PGAs from the seismograph rock sites were on average significantly smaller than those from the accelerograph rock sites. The nature of the underlying rock seemed to be an important factor, and the testing of various approaches suggested that, within the limits of the data available, a satisfactory model could be derived if three ground classes were defined as follows:

- **strong rock**; comprising classes "very strong rock" and "moderately strong rock" as described in section 6 above,
- **weak rock**; comprising the class "weak

rock" from above and the Zhao *et al.* ground class AV (bedrock of all kinds overlain by very thin (≤ 3 m) soil layer), and

• **soil**; all others.

The entire data set comprising the accelerograph data used by Zhao *et al.* (including their very near-source data from overseas earthquakes) and the seismograph data was, therefore, divided into three sets according to the new ground class definitions. The magnitude and distance ranges covered by the three sets are as shown in Figure 2(c-e).

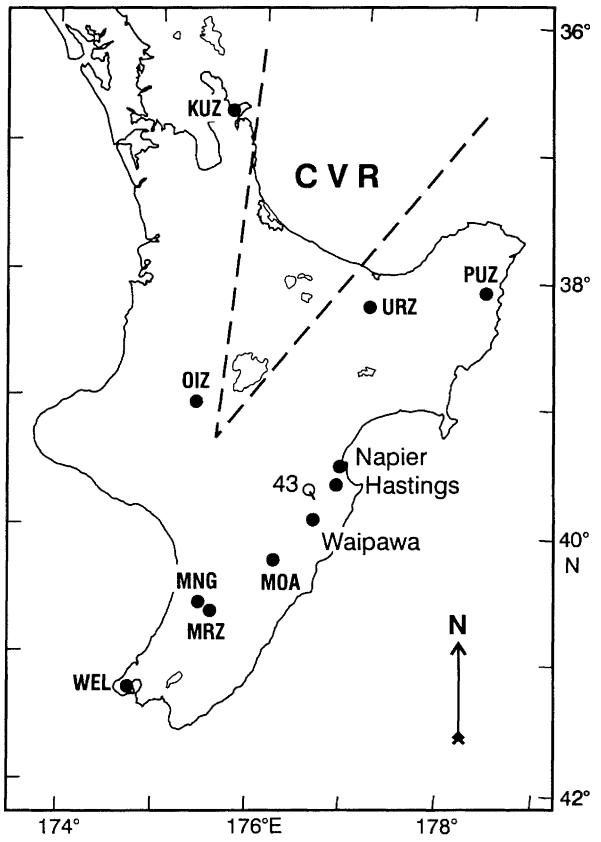

Figure 3: Locations of the Tikokino Earthquake of 11 April 1993 (event 43) and recording sites discussed in the text. The epicentre is indicated by a small circle and the horizontal projection of the fault plane by a small diagonal line. Source directivity effects gave rise to "high" PGA's at sites to the south and south-west of the epicentre and "low" PGA's at sites to the north and north-east.

7.2 Directional effects

Directional effects sometimes seemed to play a significant role. For example, PGAs from the Tikokino earthquake of 11 April 1993 showed a variation in amplitude as a function of direction that was clear in both accelerograph and seismograph data. Comparing PGAs derived from seismograms recorded at fairly similar epicentral distances at the strong-rock sites MNG, MRZ, OIZ and URZ (Figures 3, 4), the PGA values from sites MNG and MRZ located south-west of the epicentre were close to the apparent trend line for the bulk of the data, the value from site OIZ located to the north-west was a factor of about 6 below the trend line, and that from site URZ located to the north-east was below the trend line by factor of about 3. Note that site KUZ was subject to both directional and CVR effects hence the PGA value from there was very low, and also that the most direct path to site OIZ was through southern-most the tip of the CVR.

There did not seem to be any evidence in the seismogram data for frequency dependence in the variation of attenuation with direction, rather that amplitudes recorded in the low amplitude directions seemed to be reduced across the whole frequency band of interest (Figure 5).

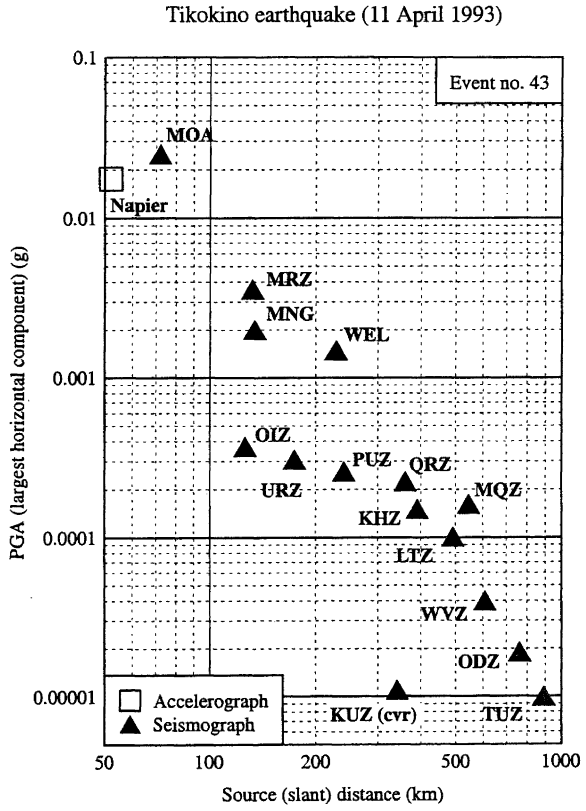

Figure 4: Illustration of directional effects using data recorded on rock sites during the Tikokino earthquake of 11 April 1993. Sites MOA, WEL and Napier are on weak rock, all others are on strong rock. Comparing the strong rock sites MNG, MRZ, OIZ and URZ, the travel paths from epicentre-to-site were respectively to the SW, SW, NW and NE. (Note that (i) travel path for KUZ was through the highly attenuating volcanic region, (ii) site MQZ often gave high PGAs for events located in the eastern North Island, (iii) sites WCZ, WLZ and RUZ (Figure 1) were not instrumented at the time of the Tikokino earthquake, and (iv) a record from site MOZ was excluded because of an instrument fault.)

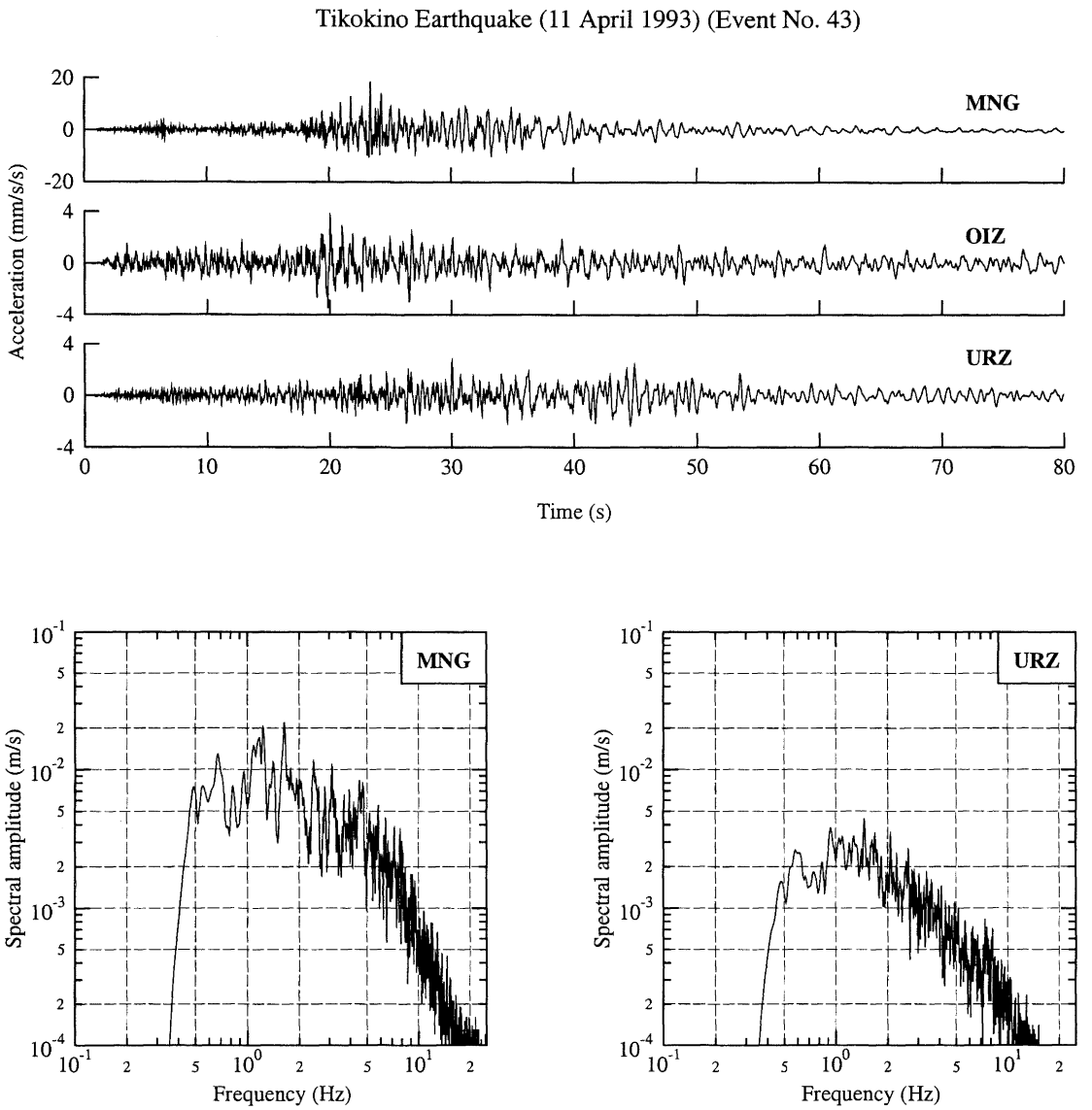

Figure 5: Time histories and Fourier spectra from the Tikokino earthquake illustrating the reduction of amplitudes over the whole frequency band of the recordings. Note the variation in Y-axis scales for the time-history plots.

Six accelerograph recording sites, namely Waipawa, Dannevirke, Napier (3) and Hastings, were within 50 km of the epicentre [6]. PGAs recorded to the south-west at Waipawa and Dannevirke were higher by a factor of about 2 than those recorded to the north-east at Napier and Hastings, after making allowance for the subsurface conditions at the sites. The accelerogram from Waipawa contained a "fault-fling" pulse of the type described by McVerry [20]. No fault-fling pulses were seen in any of the seismograph records that formed the PGA attenuation dataset.

It seems likely that the relative amplitudes of the Tikokino recordings are at least in part a consequence of source-directivity effects. Abercrombie and Benites [1] have shown that a southward rupture on the fault plane could account for the variations in the accelerograph data, and it seems reasonable to extend their reasoning to account for the south-west / north-east variations in seismograph data (comparing sites MNG and MRZ with site URZ).

Direction-dependent attenuation seemed to be indicated by data from several other earthquakes of the seismograph dataset but, as noted by Smith [26] in studies of MM Intensity attenuation, the directions of "high" attenuation varied in different regions of New Zealand. Assuming that the directional effect could be regarded as a relatively high level of attenuation along some paths, the following patterns were noted:

- for earthquakes centred in the north-west part of the South Island, PGA's from sites on the east coast of the South Island (ODZ, MQZ, LTZ and KHZ) showed signs of relatively high attenuation,
- for earthquakes centred near Cape Palliser some sites in the south-west (KHZ, LTZ, but not WVZ) indicated relatively high attenuation, and

- for earthquakes on the east coast of the North Island, from Castlepoint to Gisborne, recording sites in the north west, excluding those screened by the CVR, suggested relatively high attenuation.

The above patterns are consistent with the orientations of the elliptical isoseismal lines modelled by Smith [26], and in some of the cases where the strikes of the fault ruptures were known, also consistent with the model of Dowrick and Rhoades [11]. There were, however, many inconsistencies in the data and this, coupled with our belief that we had insufficient data for a rigorous study of the directional effects, led to a decision not to attempt to model the effects but rather to simply note that they existed.

7.3 Effect of the Volcanic Region

It has long been claimed that seismic waves propagating through the volcanic region of the North Island are subject to anomalously high attenuation [11, 13 ,18 ,24]. Note that here we are using the term "volcanic region" rather than CVR or TVZ because one of the topics for investigation is the boundary of the anomalous zone. Zhao *et al.* [30] excluded data that might have been affected by the anomalous attenuation from the derivation of their model and simply showed that such data did indeed have a mean value significantly lower than the mean value of the remaining data. Nineteen of the accelerograph records were affected.

Thirty-six records from the weak-motion NSN data set, 11% of the total, seemed to be affected by the anomalous attenuation. Symptoms were greatly reduced amplitude and less high-frequency content in comparison with "normal" records (Figures 6 and 7). The reduction in amplitude was quite dramatic, as illustrated by PGAs resulting from the Offshore East Cape earthquake of 5 Feb 1995. The most direct travel paths to sites KUZ, WLZ, OIZ and MRZ were through the volcanic region, and the PGAs recorded at those sites were approximately an order of magnitude below those recorded at similar source distances at the "normal" sites (Figure 6). Note that the PGA from site MOA can probably be regarded as higher than normal for the seismograph dataset because, as is discussed later, MOA is underlain by rock of weak strength, and also that sites WCZ and RUZ (Figure 1) were not instrumented at the time of the 5th February 1995 earthquake.

A detailed explanation of the anomalous attenuation is beyond the scope of the present paper. Suffice it to say that a selective attenuation of the high frequency components of the seismic signal may be a major reason. Low frequency components, 0.5 to 0.7 Hz (Figure 7) did not appear to be highly attenuated during passage through the volcanic region, whereas higher frequency components did.

Our first task in modelling the effect was to define the boundaries of the anomalous region. We considered three models of the volcanic region proposed previously for other purposes, namely the "CVR", the "whole TVZ", and the "young TVZ", where "CVR" stands for "Central Volcanic Region" and "TVZ" for "Taupo Volcanic Zone" [27]. The CVR (Figure 8) is a somewhat arbitrary wedge-shaped zone with its apex at Mt Ruapehu and the eastern and western sides respectively passing through Whakatane and close to the Coromandel Peninsula. The "young" and "whole" TVZs in contrast have boundaries that closely follow various known volcanic centres. They have common eastern and southern boundaries, but the whole TVZ extends further to the north-west than does the young TVZ. The young TVZ encompasses volcanic centres thought to have been active during the last 340,000 years, and for the whole TVZ those active during the last 2 million years [27].

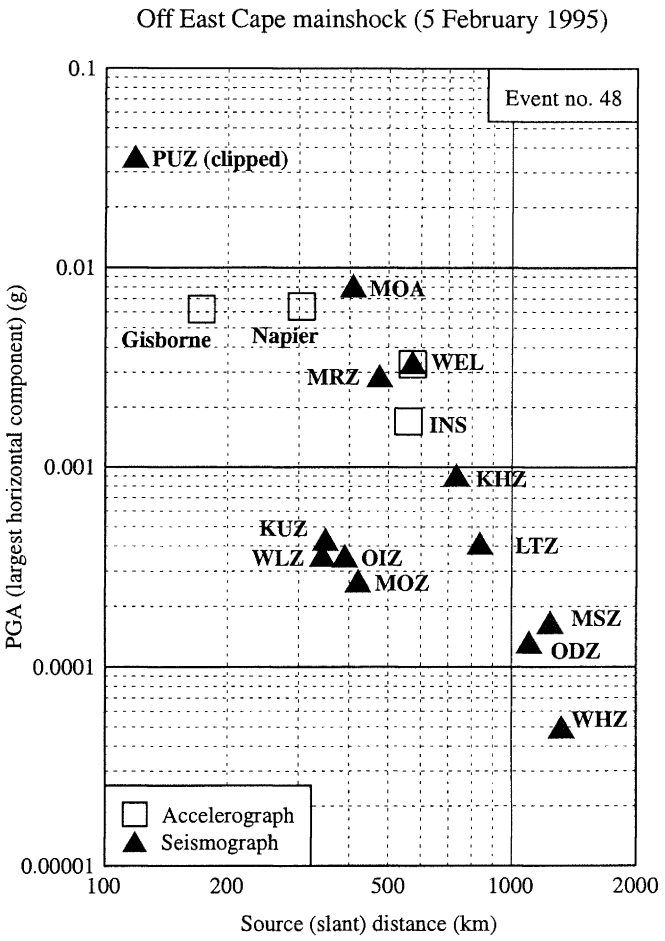

Figure 6: ***Example of high attenuation in the volcanic region of the North Island. The direct travel paths from the 5 February earthquake to sites KUZ, WLZ, OIZ and MOZ were all through the volcanic region, and the PGAs were clearly very much reduced in comparison to those recorded at locations not affected by volcanic paths. All of the recording sites were on rock.***

As a way of selecting the "best" boundaries for the anomalous region we first derived an attenuation model using records that appeared not to have passed through it. We then used that "normal" attenuation model to estimate PGAs for those records that did appear to be affected by the volcanic region, and examined the ratio "recorded/estimated" PGA as a function of direct path length through each of the model zones. Only those paths which we considered to be well defined were included in the analysis. By "well defined" we

mean that the angles of incidence at any of the boundaries were greater than about 30° so that we could safely ignore the effects of refraction at the boundaries. In time a more sophisticated model that takes into account other factors such as refraction will be developed, but that is beyond the scope of the present paper. Records with source-to-site distances greater than 400 km also were excluded.

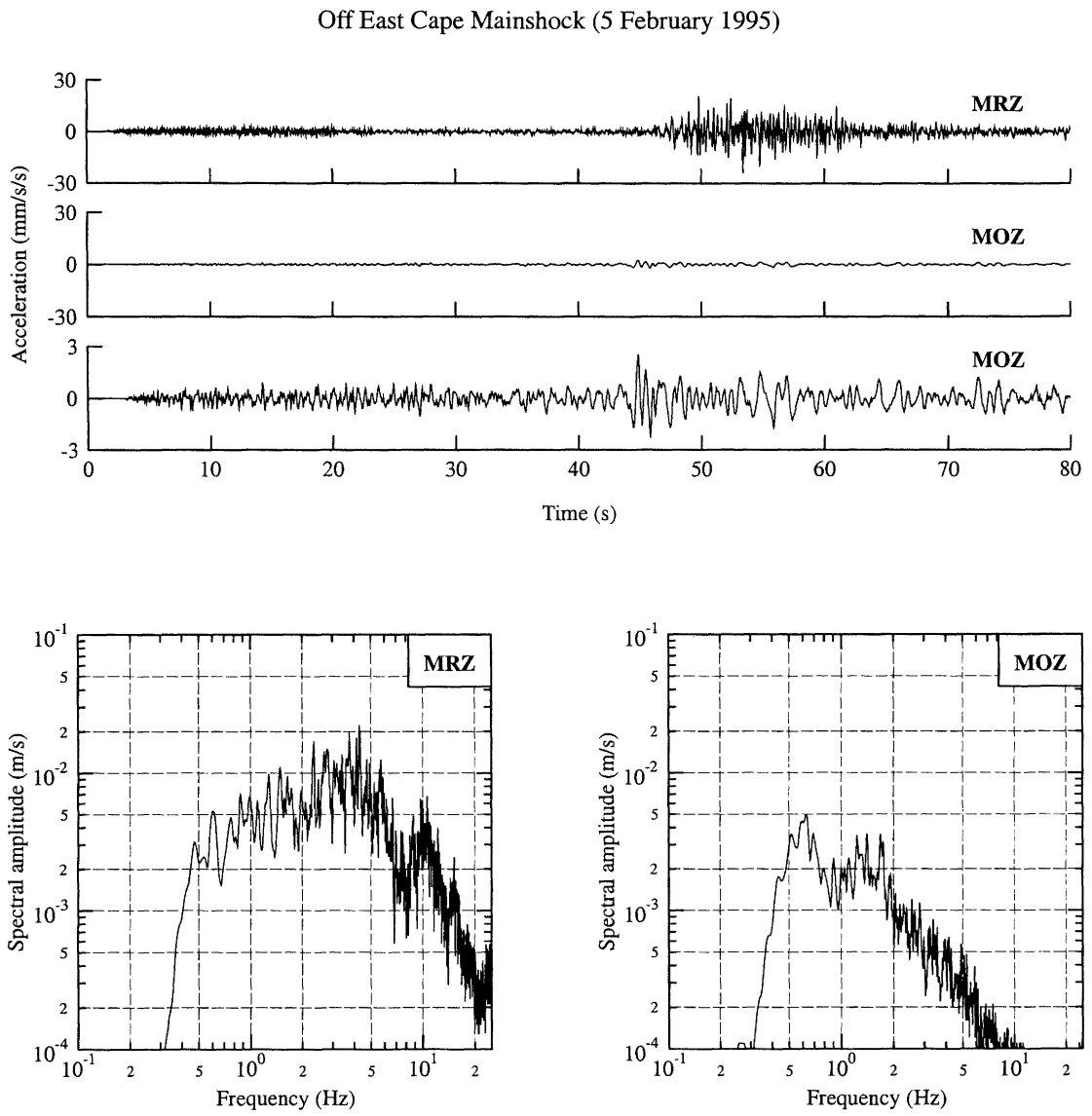

*Figure 7: **Time histories and Fourier spectra from the Off East Cape earthquake of 5 February 1995 illustrating the selective reduction of high frequency components in the seismic signal that had passed through the volcanic region. The effect is clearly evident even in the time-histories. Note the variation in Y-axis scales for the time-history plots.***

The results, Figure 9, provided some useful guidance, as follows.

- The CVR model (Figure 9(a)) gave a mean PGA ratio that first increased and then decreased as the apparent path length was increased. This seemed less realistic than for the other two models where the PGA ratio steadily decreased with increasing path length.
- The points labelled "A" in Figure 9(a), which are associated with the paths labelled "A" in Figure 7, seemed as a group to have somewhat below-average PGAs, indicating at least a moderate length of path within a highly attenuating zone. This suggests that the two TVZs provide a better southern boundary for the highly attenuating zone than does the CVR.
- Some of the data points labelled "B" in Figure 9(a) are associated with event 47 (point "B" in Figure 8).

The group average ratio of about 1 suggests a non-volcanic location for the event, which is a point in favour of the eastern boundary of the TVZ rather than that of the CVR as an eastern boundary to the anomalous zone. Event 47 was well recorded by permanent stations in the New Zealand seismograph network, and also by two additional 3-component EARSS:L4C instruments and two arrival time detectors that had been deployed temporarily in the eastern Bay of Plenty. Hence the uncertainty in the location of event 47, estimated to be about 5 km in the north-south direction and less than 5 km east-west, is better than average for events in the Bay of Plenty (T. Webb, personal communication 1999).

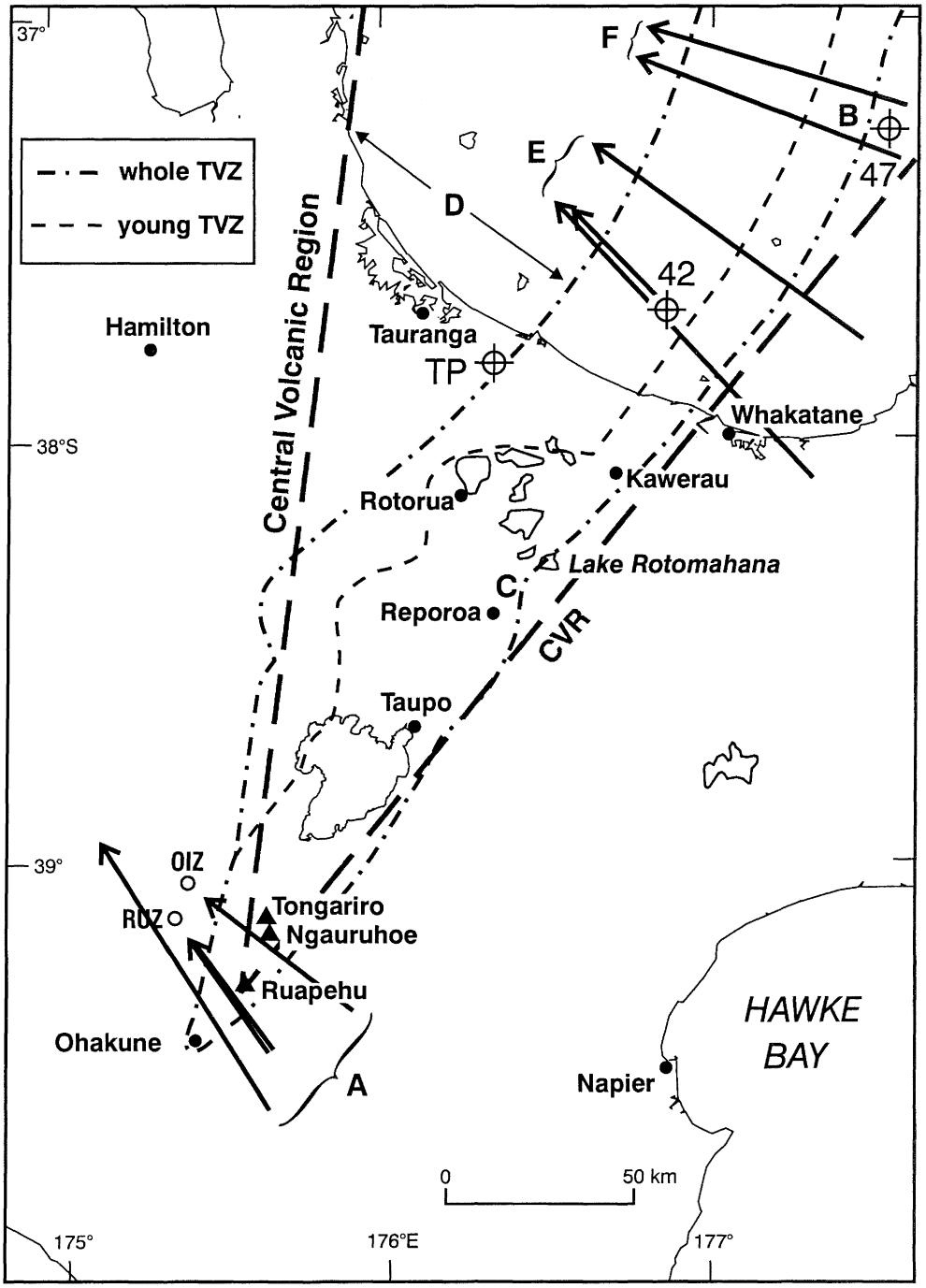

Figure 8: ***Three possible outlines for the zone of high attenuation (map adapted from Wilson et al. [27]). The labelled paths and locations, which have corresponding labelled data points in Figure 9, can be used to help define the most likely boundaries of the zone of high attenuation. The reasoning is given in the text.***

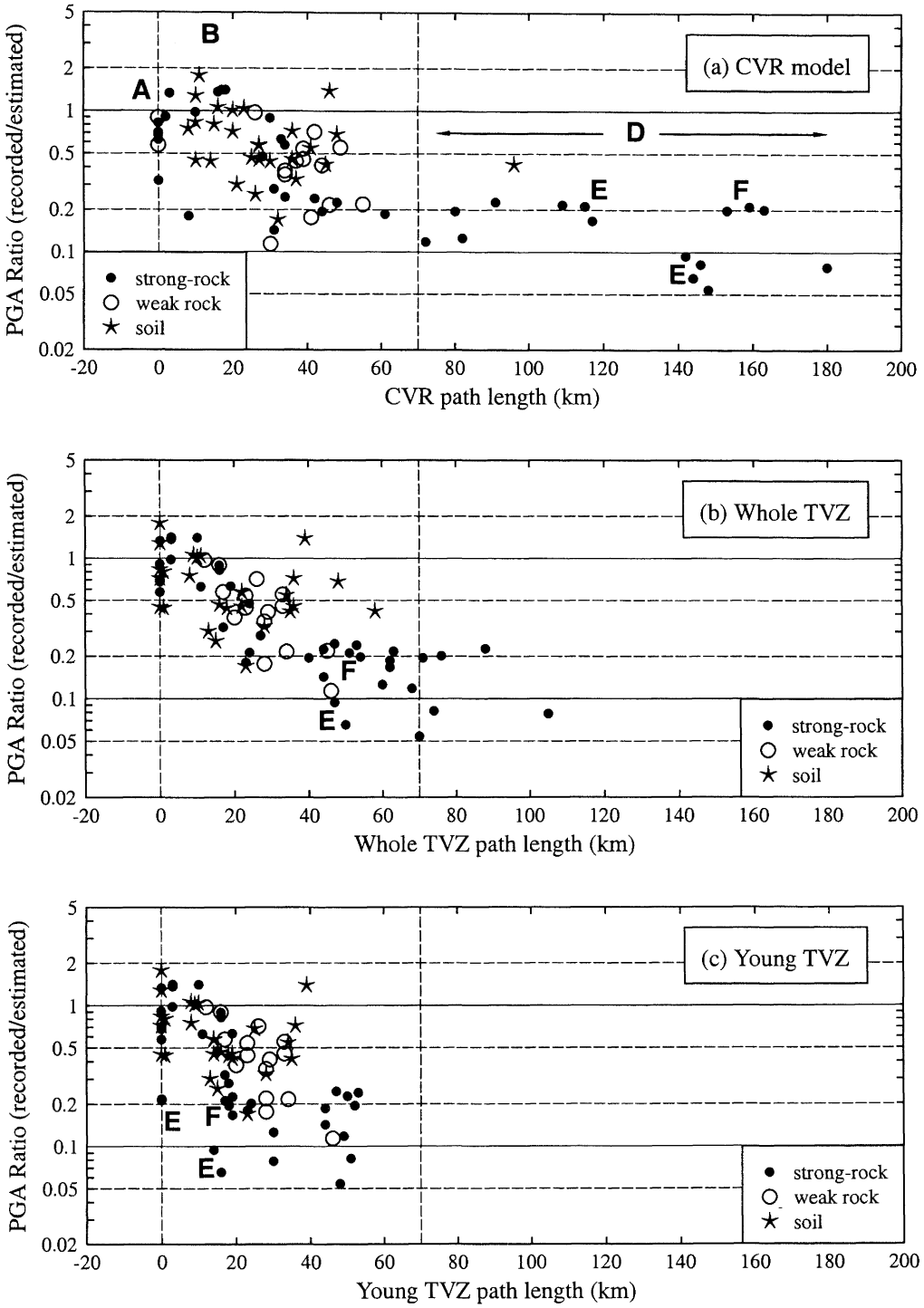

Figure 9: ***Reduction in PGA with length of path through each of the three volcanic zone models. The estimated (or reference) PGAs were calculated using an attenuation model that did not make any allowance for the high attenuation within the volcanic zones. Problems with the CVR model are (i) the depressed level of mean PGA at 0 km, (ii) the increase in PGA from 0 to 20 km, (iii) the comparatively large degree of scatter, and (iv) the "flattening out" at distances above 70 km. The main problems with the young TVZ model are (i) the large degree of scatter in the data, and (ii) some very low values of recorded PGA at 0 to 20 km. Note that the "high" soil site PGA values at about 45 km in Fig. 8(a) and 38 km in (b) and (c) were from one site in one event, suggestive of a site-specific effect. This data point was excluded from the model development.***

- Other of the data points at "B" in Figure 9(a) were obtained from recording sites between Reporoa and Lake Rotomahana ("C" in Figure 8), and again the group average PGA ratio of about 1 indicates a small or zero path within the anomalous zone. This further supports the TVZ boundary as the eastern boundary to the anomalous zone.

- Most of the points labelled "D" in Figure 9(a) were associated with paths through the wide part of the CVR in the vicinity of Tauranga. The apparent "tailing off" of the high attenuation effect at path lengths greater than about 70 km could be explained either by a lessening of the high attenuation in the portion of the CVR near Tauranga, or more simply by taking the boundary of the whole TVZ as the northwestern boundary for the anomalous zone. The exact position of the boundary remains uncertain, however, because Dowrick and Rhoades [11] noted high attenuation in the intensities of the 1976 Te Puke earthquake ("TP" in Figure 8). The instrumental epicentre for the Te Puke earthquake was located approximately 2 km west of the whole TVZ boundary, but there were some inconsistencies. The isoseismal pattern [10] seemed to imply better transmission of the seismic waves towards the east into the zone of high attenuation than towards the west. Indeed the highest isoseismal, MMI VII, lay entirely to the east of the epicentre.

- The three points labelled "E" in Figure 9(c) (paths "E" in Figure 8) appear to indicate that the young TVZ is not a good model for the north-western boundary. The two paths and points labelled "F" tend to support this view, as do the findings of Dowrick & Rhoades [11] which suggest that the zone of high attenuation extends to somewhere between Tauranga and the western boundary of the whole TVZ.

Based on the above our preferred model for the highly attenuating zone is the whole TVZ, even though some of the evidence we have provided is a little tenuous and not entirely consistent.

7.4 Development of the attenuation model

In the accelerograph dataset nearly all of the distant records are from digital instruments. Because the non-triggering of some digital instruments could bias the dataset at large distances we have estimated the trigger levels of all of the digital accelerographs and excluded from the analysis those accelerograph records obtained from distances greater than that of the first non-triggered digital accelerograph having a similar triggering level.

Most of the accelerograph records are from weak rock and soil sites within 300 km of source while many of the seismograph records are from weak and strong rock sites at source distances of more than 300 km. In order to minimise any biasing that might arise from such a grouping of the data, i.e., most soil site data at intermediate distances versus most rock site data at long distances, the maximum source distance for data used in the derivation of the model was set at 400 km. Beyond 400 km, the predicted strong motion parameter would be relevant only to unusual engineering applications and only for every large earthquakes, for example, 8.0+, and our data set does not contain any records from such large magnitude earthquakes.

Much New Zealand data is from two types of earthquakes, namely crustal and slab, and a small amount is from subduction zone interface earthquakes. It has been demonstrated that different types of earthquakes can lead to different attenuation characteristics [2, 11, 29] and so ideally a separate attenuation model should be derived for each type. Another important aspect of attenuation modelling is site effects. As described earlier most of the New Zealand accelerogram data is from soil sites. In the present study we found that data from strong rock, weak rock and soil sites exhibited significantly different PGA attenuation characteristics, and again ideally a separate attenuation model should be developed for each site class. The division into earthquake types and site classes would thus result in six major data groups, strong rock, weak rock and soil for both crustal and slab earthquakes. Such a division of the data would, however, result in a very small number of data points in each group and it would be very difficult to derive a robust attenuation model for each group.

An alternative approach could be to modify an existing attenuation model derived from a much larger overseas data set, as is being done for attenuation modelling of acceleration response spectra [21]. A difficulty with this approach is that the site classes used in the New Zealand attenuation studies are considerably different from those used in some overseas models. For example, rock sites and shallow soil sites were combined into a single rock class in one model [2], and a second model that utilised strong rock and weak rock classifications restricted the source distance to just 60 km [5]. The New Zealand dataset has very few records in that distance range (Figure 2(c-d)).

The approach that we have adopted is to combine all the data and use it to derive a single attenuation model, with some of the parameters of the model being applied to a single type of earthquake and some to a single class of site conditions. For different groupings of the data we aimed to have as many common parameters as possible so that they could be estimated from a large number of data points.

The relative lack of near-source data from even moderate magnitude earthquakes in our dataset meant that we were not confident of being able to support a model with magnitude and distance saturation characteristics, hence we followed the approach of Zhao *et al.* [30] and adopted a simple Joyner and Boore [16] type approach. Our base model was the soil site model from Zhao *et al.* [30], i.e.

$$\log_{10}(PGA_{SL}) = A_1 M_W + A_2 \log_{10}(R) + A_3 h_C + A_4 + A_5 \delta_R + A_6 \delta_I, \quad (1)$$

and

$$R = \sqrt{(r^2 + d^2)}, \quad (2)$$

where PGA_{SL} is the peak ground acceleration (g) for soil sites, M_W is the moment magnitude, r (km) is the shortest distance

from the rupture surface to the recording site, d is a constant to restrain the near-source PGA prediction and h_C (km) is the centroid depth of the rupture surface.

The dummy variables are defined as

$$\delta_R = 1 \text{ for crustal reverse faulting, otherwise 0, and}$$
$$\delta_I = 1 \text{ for interface events, otherwise 0.} \quad (3)$$

For weak rock sites, experimentation with various possibilities suggested the following form:

$$\log_{10}(PGA_{WR}) = \log_{10}(PGA_{SL}) + B \log_{10} R + C_{RK} R + D_{WR}, \quad (4)$$

and for strong rock sites

$$\log_{10}(PGA_{SR}) = \log_{10}(PGA_{SL}) + B \log_{10} R + C_{RK} R + A_{SR} M_W + D_{SR}. \quad (5)$$

For sites where the direct seismic wave path had a path length R_V (km) within the highly attenuating volcanic region, two additional distance terms were assumed for all site conditions:

$$\log_{10}(PGA_V) = \log_{10}(PGA) + B_V \log_{10}(R_V) + C_V R_V. \quad (6)$$

Parameter selection was based on the residual analysis from the present data set with respect to the attenuation models of Zhao *et al.* [30] and regression analysis for the present model was carried out. Statistical analysis was then performed for each parameter and any parameter for which the mean was not larger than zero at a significance level of 5% was excluded. It was thus found that both B and D_{WR} could be eliminated, and for the TVZ data only one of the parameters B_V and C_V could be included. Taking B_V as zero gave a much better fit to the data than taking C_V as zero. This is consistent with the findings of Haines [13] and also consistent with a physical model involving a large anelastic attenuation within the volcanic region.

The final model developed from equations 1 to 6 is:

$$\log_{10}(PGA) = A_1 M_W + A_2 \log_{10}(R) + A_3 h_c + A_4 + A_5 + A_6 + A_7 R + A_8 M_W + A_9 + A_{10} R_V$$

Where $R = \sqrt{(r^2 + d^2)}$.

Values of the parameters are as follows:

A_1	= 0.2955	(magnitude (M_W) term for all sites)
A_2	= -1.603	(geometric attenuation term for all sites)
A_3	= 0.00737	(depth term for all data)
A_4	= -0.3004	(constant term for all sites)
A_5	= 0.1074	(for crustal reverse faults only, otherwise 0)
A_6	= -0.1468	(for interface events only, otherwise 0)
A_7	= -0.00150	(anelastic attenuation term for strong and weak rock sites only)
A_8	= 0.3815	(additional magnitude term for strong rock sites only)
A_9	= -2.660	(additional constant term for strong rock sites only)
A_{10}	= -0.0135	(additional anelastic attenuation for paths through the TVZ)
d	= 19.0	(factor for near-source constraint)

$\sigma_{\log10(PGA)} = 0.24$

Residuals from the modelling are plotted in Figures 10 to 12, some sample fits for individual earthquakes are plotted in Figure 13, and the general form of the model is shown in Figure 14.

8.0 DISCUSSION

The total magnitude term for the strong rock class is much larger than for the other site classes. Part of the reason for the large value could be associated with a strong anti-correlation between the coefficient for the additional strong rock magnitude term, A_{SR}, and the strong rock constant D_{SR}, indicating that a smaller pre-defined value for A_{SR} could result in a model with very similar predictions within the magnitude range of the data. This strong correlation suggests that extrapolation outside the magnitude range of the dataset (i.e. M_W 5.08 to 7.41) could result in unreliable predictions.

We attempted to derive a model with magnitude-dependent geometric attenuation to ensure that the large magnitude term for strong rock sites was not caused by the assumption of magnitude-independent attenuation. It was found that the coefficient for the magnitude-dependent attenuation term was not statistically significantly larger than zero and was too small to have any effect on the model's predictions. We also attempted to fit a model with a magnitude-dependent "d" (equation 2) using fixed coefficients from Campbell [4], and found that the fitted model had a very similar value for the magnitude term to that given above. Figure 10 shows that there is no strong dependence on magnitude or distance for residuals of strong rock site data. These analyses suggest that the large value of the magnitude term is either a result of a particular distribution of our data or a result of physical characteristics of the New Zealand earthquakes. Note that the magnitude term for the soil and weak rock data is also larger than those of Joyner and Boore [16].

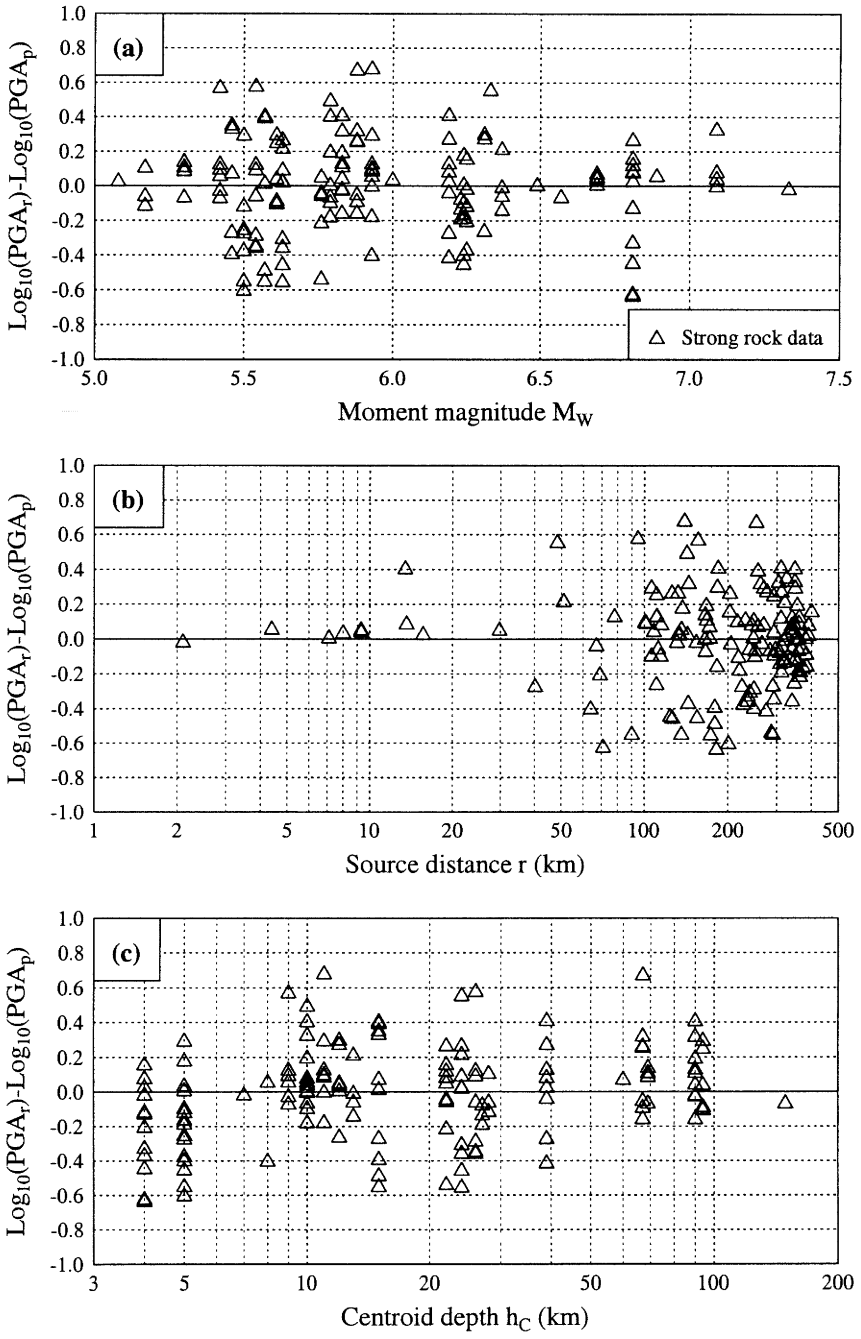

Figure10: Residuals of the PGA data from strong-rock sites plotted against (a) moment magnitude M_w, (b) source distance r, and (c) centroid depth h_c. PGA_r is the recorded PGA and PGA_p is the predicted PGA. A positive residual means that the recorded PGA is greater than the predicted PGA. The apparent over-prediction at centroid depths of 4 and 5 km in plot (c) is probably a result of directivity effects associated with the shallow events 39, 46, and 51. See for example Figure 13(a).

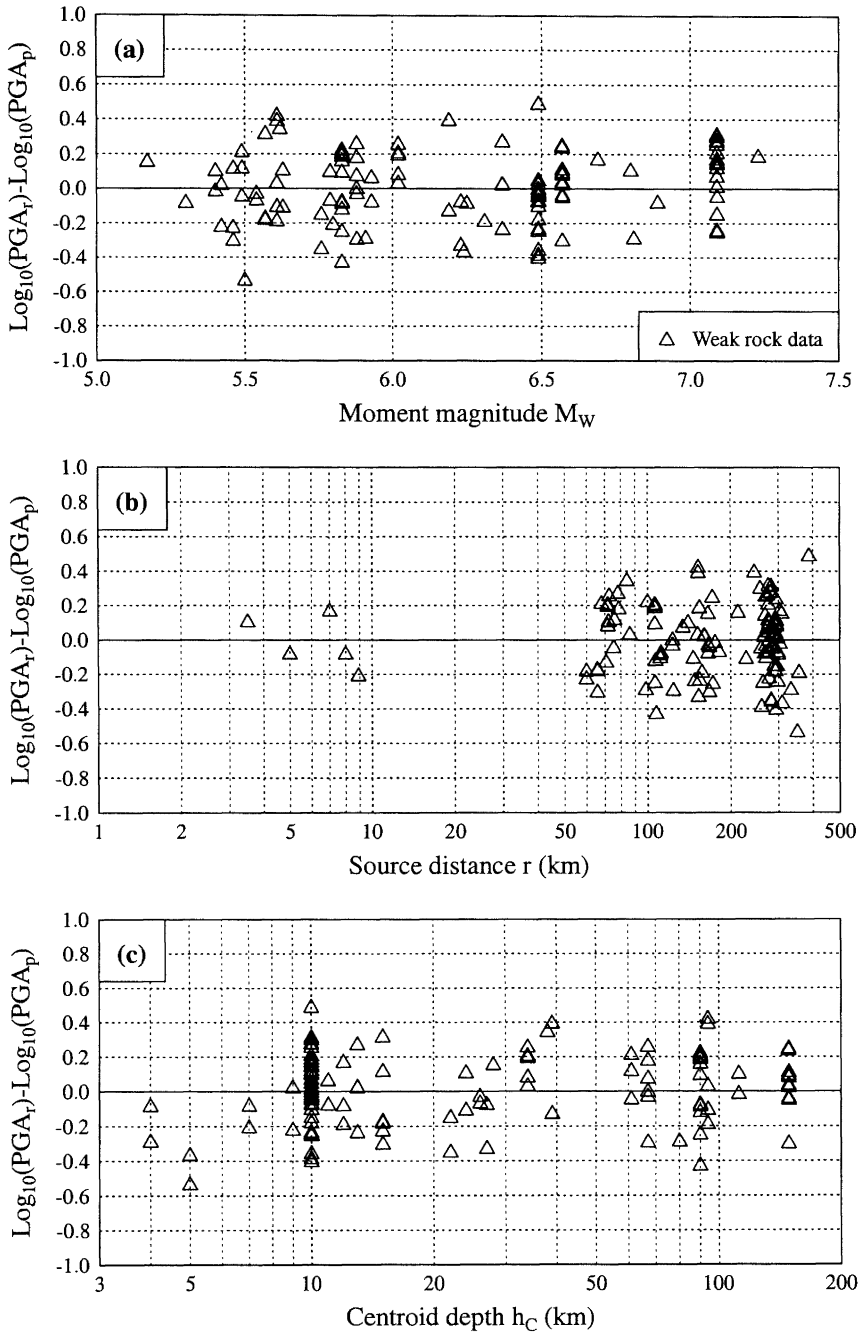

Figure 11: Residuals of the PGA data from weak-rock sites plotted against (a) moment magnitude M_w, (b) source distance r, and (c) centroid depth h_c. PGA_r is the recorded PGA and PGA_p is the predicted PGA. The apparent over-prediction at centroid depths of 4 and 5 km in plot (c) is probably a result of directivity effects associated with the shallow events 39, 46 and 51.

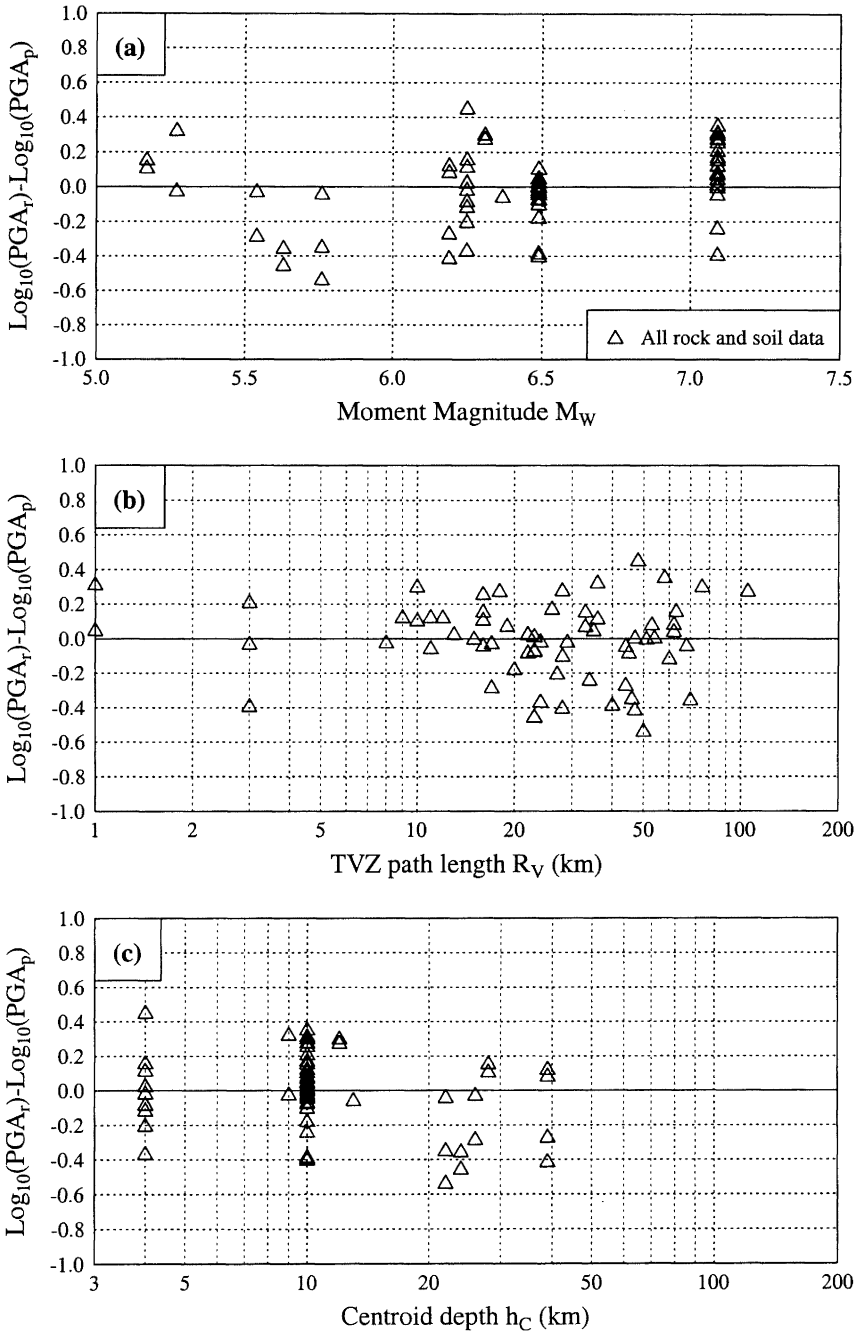

Figure 12: Residuals of PGA data affected by paths through or within the TVZ. Results for all rock and soil sites are plotted against (a) moment magnitude M_w, (b) length of path in the TVZ R_v, and (c) depth h_c. PGA_r is the recorded PGA and PGA_p is the predicted PGA.

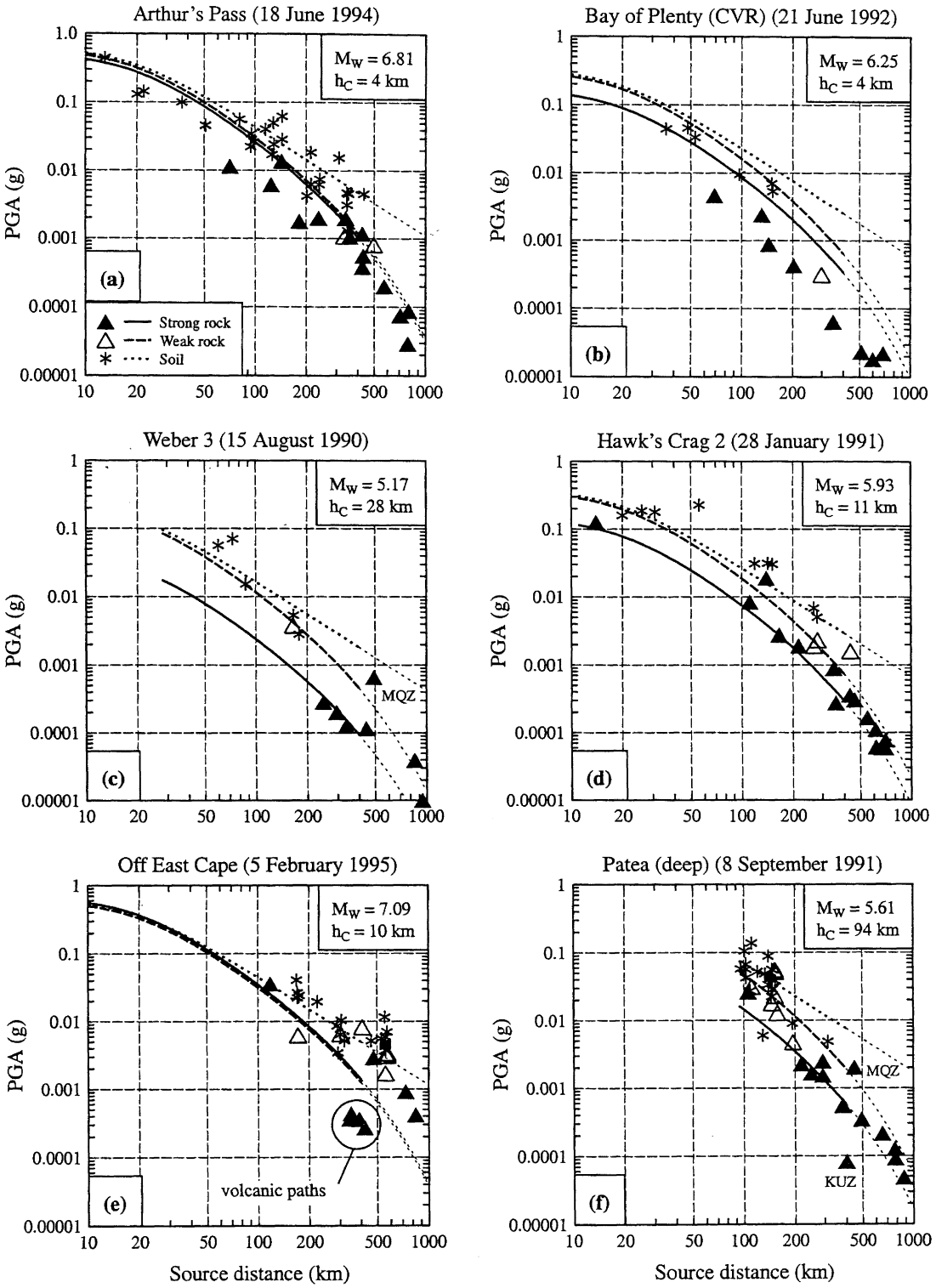

Figure 13: Comparisons of recorded and modelled PGAs for 6 New Zealand earthquakes. The plotted curves do not include the volcanic path factor, and the data is from accelerograph and NSN sites only. (a) The Arthur's Pass earthquake of 18 June 1994, showing good agreement apart from depressed values of PGA recorded on the Christchurch side of the epicentre - probably a directional effect. (b) An event located within the volcanic region showing general over-prediction by the version of the model not incorporating the volcanic path factor. (c) A magnitude 5 event (noting that the "high" strong rock PGA was recorded at site MQZ which often gave high results for events located northwest of the site). (d) An event with magnitude close to 6. (e) A magnitude 7 event (the worst fit for all events in the digital data set). (f) The deepest event in the seismograph dataset (the record from site KUZ showed symptoms of a volcanic path even though the direct path was not through the whole TVZ).

The residual distribution with depth for strong rock sites (Figure 10(c)) apparently has a small trend, with records from very shallow earthquakes ($h_C \leq 5$ km) being over-predicted and those from deep earthquakes being marginally under-predicted. We do not think this is a real trend because much of it can be explained by the fact that three of the shallowest events (39, 46 and 51, Table 2) were located in the centre of the South Island, and directional effects seem to have resulted in depressed PGA values at recording sites in the sector defined by a line extending north-east of the epicentres and then clockwise to approximately south. Sites ODZ, MQZ, LTZ and KHZ were involved.

Similarly the same three events were associated with all three of the shallow-event ($h_C \leq 5$ km) records that were over-predicted by more than one standard deviation in the weak-rock case (Figure 11(c)). In this case only one recording site, WEL, was involved and it was located north-east of all three events. A fourth over-predicted record, at $h_C = 9$ km, also was from site WEL which once again was approximately north-east of the earthquake, event 35. The two common factors make it impossible to determine whether the over-prediction is due to (i) an overall trend in the data, (ii) a site effect, or (iii) a directional effect. There is clearly a need for much more data from weak rock sites.

If a separate depth term was allowed for the strong rock case, then the trend in the residual distribution with depth could be corrected and also the coefficient for the depth term for the strong rock site would be statistically larger than zero. However, this would result in a much larger magnitude term for the strong rock case and an almost perfect anti-correlation between A_{SR} and D_{SR}. A separate depth term for strong rock sites was, therefore, not included in the model presented here.

The remaining very shallow event, the 4 km deep M_W 6.25 Bay of Plenty (CVR) earthquake of 21 June 1992, was well predicted by the complete model including the volcanic path term (Figure 12(c)), whereas all records were clearly substantially over-predicted by the model when the volcanic path term was not included (Figure 13(b)).

Single event plots for the smallest, a mid range, and the largest crustal events, and the deepest event in the seismograph dataset are shown in Figure 13(c-f). In all cases the model, without the volcanic path term, is plotted with heavy lines over the distance range of the data used in its development, i.e. up to 400 km, and with light dashed lines for extrapolations to 1000 km. The fits are good, accepting the usual level of scatter in PGA data, even for distances beyond 400 km. A notable exception however is the fit to the M_W 7.09 Off East Cape earthquake of 5 February 1995. For this earthquake the model under-predicts the non-volcanic path data recorded on rock sites at distances above about 300 km. We do not have an explanation for this and simply note the need for more data from events of similar or larger size.

The two next largest events in the seismograph dataset, Secretary Island, Fiordland (10 August 1993) and Arthur's Pass (18 June 1994), both had a moment magnitude of 6.81. The agreement between predicted and recorded PGAs on rock sites for the Secretary Island event was excellent for distances from 100 to 600 km. From 600 to 1200 km the model underestimated the recorded PGAs by a factor of about 2. In the case of the Arthur's Pass earthquake the agreement between the predicted and recorded PGAs was good, apart from those results that may have been affected by directional effects (Figure 13(a)).

The general form of the model is illustrated in Figure 14 with plots for shallow crustal events having strike-slip mechanisms. The most notable feature is the changing relativity between PGAs on strong rock sites and those on weak rock and soil sites as a function of magnitude. For a magnitude 5 earthquake the PGAs on weak rock are amplified by a factor of about 5.5 with respect to those on strong rock sites, for a magnitude 6 event the amplification factor is 2.4, and at magnitude 7 there is no significant amplification. The form assumed for our model means that the amplifications apply at all source distances. This trend is supported by the recorded data as shown for example in Figure 13. It should be noted however that there is very little rock data at distances less than 50 km, and only 9 records from rock sites at distances less than 100 km from earthquakes of magnitude 6.5 and above. At magnitude 8, a large extrapolation, the model predicts attenuation by a factor of about 2.5 from strong rock to weak rock and soil sites. Verification of this prediction awaits data.

PGAs predicted for soil sites are very similar to those for weak rock sites for source distances up to about 50 km. At distances beyond 50 km there is significant amplification on going from weak rock to soil and the amount of amplification increases with distance. The model for soil sites (Figure 14) produces attenuation curves that are very similar to those predicted by the model of Zhao *et al.* [30], even though the parameters of the two models differ.

The predictions for near-source accelerations in large earthquakes are very high. At source distance r = 1 km a magnitude 8 event with strike-slip mechanism could be expected to yield mean PGAs of 1.14g on weak rock and soil sites, and 2.8g on strong rock sites. Such an event could be, for example, a major rupture involving the southern and central segments of the Alpine fault [28]. The predictions for a magnitude 7.5 strike-slip event and r = 1 km are 0.8g on weak rock and soil and 1.3g on strong rock at near-source locations. The southern segment of the Wellington fault is one possible source of such an event.

According to the model, events with reverse mechanism would give rise to PGAs that are 29% higher than those predicted above for strike-slip events.

All of the extrapolations to magnitude 7.5 and above need to be treated with caution as our model, like that of Zhao *et al* [30], does not allow for the possibility of "saturation" of mean PGA values at short distances in large magnitude earthquakes. It assumes a variation with magnitude that is independent of distance. There are some theoretical grounds for believing that the highest achievable PGAs for rock sites might be about 2g for events having reverse mechanisms, 0.7g for pure strike-slip, and 0.4g for normal mechanisms [19]. PGAs on soil too might be limited by non-linear stress-strain characteristics, which are accommodated in our model.

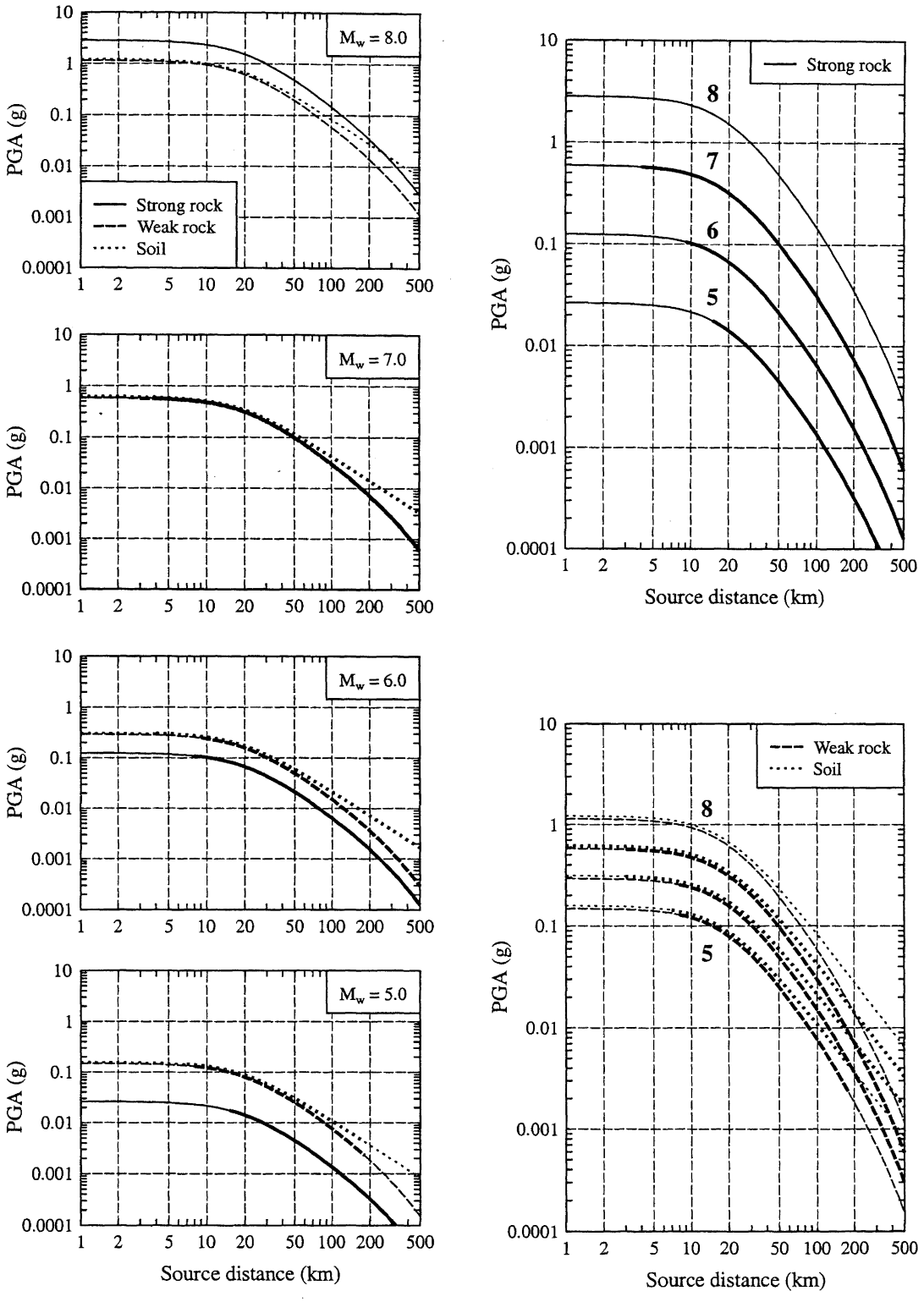

Figure 14: Predicted PGAs for shallow (h_c = 10 km) events with various magnitudes and strike-slip or normal mechanisms. Note the large amplification in PGA on going from strong rock to weak rock and soil for a magnitude 5 event, the lesser amplification at magnitude 6, the equality at magnitude 7, and the de-amplification at magnitude 8. The thin lines indicate extrapolation beyond the magnitude and distance bounds of the data used in developing the model. The magnitude 8 predictions are extrapolations, as are the very near-source predictions for magnitudes 5 and 6.

Despite the inclusion of 66 near-source records from overseas earthquakes in our dataset we still have insufficient near-source data. In Figure 14 we emphasise those parts of our model that are supported by at least some data, and the near-source gaps are obvious. See also Figure 2(c, d, e). Our model can be considered well constrained near-source only for soil sites and then only for magnitudes in the range 6.5 to 7. There is a well-recognised shortage of data for magnitudes 7.5 and above and a possibly equally important shortage of near-source data for magnitudes 5 to 6.5. Thus most near-source applications of our model, and indeed of any other of the current PGA attenuation models, should be handled with due caution.

9. CONCLUSIONS

1. Seismograph data have proven to be a valuable complement to accelerograph data for modelling the attenuation of peak ground acceleration. Using a combination of seismograph and accelerograph data we have extended the PGA attenuation model of Zhao, Dowrick and McVerry [30] to include the additional site category of strong rock, and also have successfully modelled the relatively high attenuation in the volcanic zone of the North Island of New Zealand.

2. Three ground classes, namely strong rock, weak rock and soil, were found to give rise to significantly different PGAs. As defined the "strong rock" class included rock types such as unweathered granite, schist, quartz and greywacke, the "weak rock" class included sandstones and mudstones, weathered rock of all types, and bedrock of all types overlain by up to 3 m of soil, and the "soil" class included soils of all types at depths of more than 3 m over bedrock.

3. PGAs predicted for soil sites were very similar to those predicted by the model of Zhao *et al.* [30] for all magnitudes, depths and distances.

4. The PGAs predicted by the model for sites underlain by weak rock types and soils were similar, regardless of magnitude, for source distances up to 50 km. Beyond 50 km the PGAs on soil sites were greater than those on weak rock sites and the difference increased with distance.

5. There was a magnitude-dependent amplification of PGA on going from strong rock sites to weak rock or soil sites. At magnitude 7 there was no significant amplification (for source distances up to 50 km), for magnitudes below 7 the amplification factor was greater than one with the degree of amplification increasing as the magnitude decreased, and for magnitudes greater than 7 the amplification factor was less than one, i.e. attenuation.

6. Very close to the source (i.e. within about 2 km) of earthquakes having strike-slip or normal mechanism the model predicted PGAs for weak rock and soil sites that increased with magnitude, from 0.15g at magnitude 5 to 1.2g at magnitude 8. Near-source PGAs on strong rock sites showed a greater variation with magnitude, from a little under 0.02g at magnitude 5 to 2.8g at magnitude 8. It should be noted however that the largest event in the combined weak- and accelerograph datasets had a magnitude of 7.4, and so the predicted PGAs for a magnitude 8 event are based on extrapolation and therefore must be treated with caution.

7. PGAs predicted for events having a reverse faulting mechanism were 29% greater than those predicted for strike-slip or normal mechanisms, for all distances and site categories.

8. The PGA attenuation model is applicable to all of New Zealand including the zone of relatively high attenuation in the volcanic region of the North Island. Within the anomalous zone there appears to be a much higher level of anelastic attenuation than in the rest of New Zealand, with the result that the PGA amplitude is reduced by a factor of 10 for seismic waves passing completely through it at its widest part. The maximum effective width appears to be about 70 km. The extra attenuation is modelled well by a simple function of the length of path within the anomalous zone.

9. The whole Taupo Volcanic Zone (TVZ) appears to be a better model for the extent of the highly attenuating volcanic zone than either the CVR (Central Volcanic Region) or young TVZ models.

10. There is an indication that the high attenuation within the TVZ is due to selective attenuation of some frequency components of the seismic signal. Components of 1 Hz and above appear to be much more highly attenuated than components below 1 Hz.

11. Outside of the TVZ, directional effects were observed to be substantial, but we had insufficient data for reliable modelling of the effects.

12. The ranges of validity of the model as defined by the data used in its generation are as follows: moment magnitude 5.1 to 7.4, source distance c.10 to 400 km, and centroid depth 4 to 149 km. As is common for PGA attenuation studies there was a relative scarcity of near-source data from large events, i.e. data from within 10km source distance of events of M_W 7.5 and greater. Our data set for example contained only one record from rock sites at distances less than 150 km for magnitudes 7.0 and above. There was an equally important lack of near-source data for smaller magnitudes in the range 5 to 6.5. In summary, the near-source constraint of our model should be considered adequate only for the soil ground classification and even then only for the magnitude range 6.5 to 7. All other near-source predictions are extrapolations beyond the range of data used in defining the model and should be treated with due caution.

10. ACKNOWLEDGMENTS

We gratefully acknowledge the valuable contributions made by many others to our work: Nick Ambraseys of Imperial College, London, for suggesting to our colleague David Dowrick that we explore the use of PGAs derived from seismograms; David Dowrick, Graeme McVerry, Mike Kozuch and an anonymous reviewer for very helpful reviews and suggestions; Terry Webb for providing the seismograph data; Steve Sherburn, Fred Langford and Tony Hurst for information on the site conditions for the TVZ seismograph array, and Ray Maunder for information on the site conditions for the NSN instruments. A special acknowledgement is due to the Earthquake Commission, Wellington, who over the last decade have funded most of the digital accelerographs and seismographs in our networks. Without their support this paper would not have eventuated. The work was funded by the New Zealand Government through FRST contract C05506.

11. REFERENCES

1. Abercrombie, R.E. and Benites, R.A. (1998), Strong-motion modelling of the 1993 Tikokino earthquake, Southern Hawke's Bay, New Zealand. *NZ J Geology and Geophysics* **41**:259-270.

2. Abrahamson, N. and Silva, W. (1996), Empirical response spectra attenuation relations for shallow crustal earthquakes. *Seismological Research Letters* **68**(1): 94-117.

3. Borcherdt, R.D. (1994), Estimates of site-dependent response spectra for design (methodology and justification), *Earthquake Spectra,* **10**(4), 617-653.

4. Campbell, K.W. (1997), Empirical near-source attenuation relationships for horizontal and vertical components of peak ground acceleration, peak ground velocity, and pseudo-absolute acceleration response spectra. *Seismological Research Letters* **68**(1): 154-179.

5. Campbell, K.W. and Bozorgnia, Y. (1994), Near-source attenuation of peak horizontal acceleration from world-wide accelerograms recorded from 1957 to 1993. *Proc. Fifth U.S. National Conference on Earthquake Engineering,* Chicago.

6. Cousins, W.J., Porritt, T.E., Hefford, R.T., Baguley, D.E., O'Kane, S.M. and McVerry, G.H. (1993), Computer analyses of New Zealand earthquake accelerograms 8: the Tikokino, Fiordland, and Ormond earthquakes of 1993, *Institute of Geological & Nuclear Sciences,* Science Report 94/33, 316p.

7. Cousins, W.J., Hefford, R.T., Baguley, D.E., O'Kane, S.M., McVerry, G.H. and Porritt, T.E. (1995), Computer analyses of New Zealand earthquake accelerograms, 9: the Arthur's Pass earthquake of 18 June 1994, *Institute of Geological & Nuclear Sciences,* Science Report 95/32, 79p.

8. Cousins, W.J., Perrin, N.D., McVerry, G.H., Hefford, R.T. and Porritt, T.E. (1996), Ground conditions at strong-motion recording sites in New Zealand, *Institute of Geological & Nuclear Sciences,* Science Report 96/33, 244p.

9. Cousins, W.J. and McVerry, G.H. (1997), Peak accelerations, velocities and displacements from New Zealand earthquake accelerograms, *Institute of Geological & Nuclear Sciences,* Science Report 97/10, 62p.

10. Downes, G.L. (1995), Atlas of isoseismal maps of New Zealand. Monograph 11, *Institute of Geological & Nuclear Sciences*, Lower Hutt.

11. Dowrick, D.J and Rhoades, D.A. (1999), Attenuation of Modified Mercalli Intensity in New Zealand earthquakes, *Bulletin NZ Society for Earthquake Engineering*, **32**(2), 55-89.

12. Gledhill, K.R. (1991), EARSS user's manual, *Geophysics Division Technical Report* No. 109, DSIR Geology and Geophysics, Wellington.

13. Haines, A.J. (1981), A local magnitude scale for New Zealand earthquakes, *Bulletin Seismological Society of America,* **71**(1), 275-294.

14. Hefford, R.T., Tyler, R.G. and Skinner, R.I. (1980), The MO2A strong-motion accelerograph, *Bulletin NZ National Society for Earthquake Engineering,* **13**(4), 374-379.

15. Hodder, S.B. (1983), Computer processing of New Zealand strong-motion accelerograms, *Bulletin NZ National Society for Earthquake Engineering,* **16**(3), 234-246.

16. Joyner, W.B. and Boore, D.M. (1981), Peak horizontal acceleration and velocity from strong-motion records including records from the 1979 Imperial Valley, California, earthquake. *Bulln. Seismological Society of America* **71**: 2011-2038.

17. Mark Products U.S., Inc. Product data sheet.

18. Maunder, D.E. (Ed.) (1997), New Zealand seismological report 1995, *Seismological Observatory Bulletin E-177, Institute of Geological & Nuclear Sciences*, Science Report 97/12, 279p.

19. McGarr, A. (1982), Upper bounds on near-source peak ground motion based on a model of inhomogeneous faulting, *Bulletin Seismological Society of America,* **72**(6), 1825-1841.

20. McVerry, G.H. (1997), Near-fault earthquake records and implications for design motions, *Proceedings, Technical Conference and AGM,* 14-16 March 1997,

Wairakei, NZ National Society for Earthquake Engineering, 88-95.

21. McVerry, G.H. Attenuation of acceleration response spectra in New Zealand earthquakes. [work in progress]

22. National Earthquake Hazard Reduction Program (1995), 1994 Recommended Provisions for Seismic Regulations of New Buildings: Part 1, Provisions. *Issued by Federal Emergency Management Agency,* FEMA 222A, 290pp.

23. NZS4203:1992, Code of practice for general structural design and design loadings for buildings, *Standards New Zealand*, Wellington.

24. Pancha, A. and Taber, J.J. (1997), Attenuation of weak ground motions, *Report prepared for the New Zealand Earthquake Commission, School of Earth Sciences*, Victoria University of Wellington, August.

25. Skinner, R.I. and Stephenson, W.R. (1973), Accelerograph calibration and accelerogram correction, *Earthquake Engineering and Structural Dynamics*, **2**, 71-86.

26. Smith, W.D. (1995), A development in the modelling of far-field intensities for New Zealand earthquakes, *Bulletin NZ National Society for Earthquake Engineering,* **28**(3), 196-217.

27. Wilson, C.J.N., Houghton, B.F., McWilliams, M.O., Lanphere, M.A., Weaver, S.D. and Briggs, R.M. (1995), Volcanic and structural evolution of Taupo Volcanic Zone, New Zealand: a review. *J. Volcanology and Geothermal Research* **68**: 1-28.

28. Yetton, M.D., Wells, A. and Traylen, N.J. (1998), The probability and consequences of the next Alpine Fault earthquake. *Research Report 95/193, Earthquake Commission.*

29. Youngs, R.R., Abrahamson, N., Makdisi, F. and *Sadigh, K. (1995), Magnitude-dependent variance of peak ground acceleration. Bulletin Seismological Society of America* **85**(4): 1161-1176.

30. Zhao, J.X., Dowrick, D.J. and McVerry, G.H. (1997), Attenuation of peak ground accelerations in New Zealand earthquakes, *Bulletin NZ National Society for Earthquake Engineering,* **30**(2), 133-158.

APPENDIX 1: SITE GEOLOGY

A1.1 Accelerograph (strong-motion) "rock" recording sites

ZDM class[1]	Rock class[2]	Site Name[3]	Subsurface Geology
AR	V	Manapouri Power Station	Foliated gneiss and granite
AR	V	Cromwell Bridge (rock site)	Schist
AR	V	Te Kuha	Quartz diorite
AR	M	Lower Hutt Kiosk Substation Belmont	Greywacke (moderately strong)
AR	M	Petone Overbridge Substation	Greywacke (moderately strong)
AR	M	Tuai Power Station	Sandstone/siltstone
AT	W-M	Napier Hospital **[Napier]**	Limestone (Nukumaruan)
AT	W	Atene A (Puketapu)	Massive blue siltstone of Tertiary age
AT	W	Atene B (midway Puketapu)	Massive blue siltstone of Tertiary age
AT	W	Atene D (ridge road)	Massive blue siltstone of Tertiary age
AR	W	Lower Hutt INS DSIR **[INS]**	Greywacke, completely weathered
AT	W	Lower Hutt Naenae Reservoir	Greywacke, weathered
AR	W	Wellington. Church St Substation	Greywacke, weathered
AR	W	Wellington. Dalmuir House (basement)	Greywacke, weathered
AR	W	Wellington. Hosp Ward Spt Blk (blr rm)	Greywacke
AR	W	Wellington. Morrison Morpeth (lwr grd flr)	Greywacke, weathered
AR	W	Wellington. Reserve Bank (basement)	Greywacke, weathered
AT	W	Wellington. Seismological Obs. **[WEL]**	Greywacke, weathered
AV	W	Gisborne Pumping Station **[Gisborne]**	Mudstone beneath 3 m sand and shells
AV	W	Havelock Post Office	Chlorite schist beneath 2 m soil
AV	W	Porirua Free Ambulance Depot	Greywacke (weathered) beneath 1 m sandy clay
AV	W	Taihape Post Office	Mudstone beneath 2 m? terrace alluvium, sand, silt and gravel

Notes:

1. *Ground Classification used by Zhao et al. [30]*
   - *AR* — *rock outcrop*
   - *AV* — *bedrock with very thin (≤ 3 m) soil layer above*
   - *AT* — *sites conforming to subclasses A or AV, but also possibly subject to topographic amplification*
   - *AL* — *soil layer of thickness > 3 m overlying bedrock, with estimated site period < 0.25 s.*

2. *Ground Classification used here*
   - *V* — *rock outcrop, very strong rock*
   - *M* — *rock outcrop, moderately strong rock*
   - *W* — *rock outcrop, weak rock, plus class AV from Zhao et al.*

3. *Names in bold are as referenced in the body of the paper.*

A1.2: Seismograph recording sites - National Seismograph Network.

Rock class[1]	Site Code and Name	Subsurface Geology
M	BCZ, Braida Crags	Limestone, moderately strong, but beds are quite thin with respect to the hundreds of metres of Miocene soft rocks they form a harder part of.
M	CDZ, Cobb Dam	Schist, slightly weathered.
V	DCZ, Deep Cove	Gneiss, very strong.
M	DSZ, Denniston North	Coarse sandstone/coal measures over a basement of strong Greenland Group greywacke. Sandstone is moderately strong.
V	KHZ, Kahutara	Jurassic Greywacke. Strong to very strong and massive.
V	KUZ, Kuaotunu	Greywacke, probably weathered, strong. Few metres into horizontal mineshaft. Close to contact with ignimbrite.
W	LMZ, Lake Moeraki	Instrument in temporary location, on soil or shattered rock (exact location uncertain) at the time of the recordings.
M	LTZ, Lake Taylor	Triassic Greywacke
M	MNG, Mangahao	Greywacke
W	MOA, Motea	Limestone, usually weak and in thin beds. Most of the rock under it is grey siltstone.
V	MOZ, Mahoenui	Jurassic Greywacke, unweathered, strong. (The Awakino river has cut through the weathered profile).
M	MQZ, McQueen's Valley	McQueen's Andesite, blocky and weathered, but moderately strong. Probably not very thick, 10 s to 100 s of metres, overlying greywacke.
M	MRZ, Mangatainoka River	Greywacke, fractured, moderately strong.
V	MSZ, Milford Sound	Darran Diorite. Very strong.
M	ODZ, Otahua Downs	Low-grade schist. Moderately strong.
M	OIZ, Oio	Jurassic greywacke exposed in valley of Whakapapa River.
M	PUZ, Puketiti	Site is on Cretaceous sandstone, moderately strong. This is a thin slab thrust over younger, weaker rocks, including Whangai shale and bentonite which deform plastically, forming diapirs. The slab is in the order of 5 km by 3 km by a few hundred metres thick, overlying 1 to 2 km of the weaker rock.
		Golden Bay Schist, strong.
V	QRZ, Quartz Range	Limestone, in beds about 10 m thick, in weak mudstone 1-2 km thick. Although
W	RUZ, Raurimu	the site is limestone, the overall conditions are those of weak rock.
		Granitic rock, mapped as diorite, strong.
		Permian Greywacke, predominantly siltstone.
V	SIZ, Stewart Island	Haast Schist (low grade). Weathered in top 10 to 20 m.
M-V	THZ, Tophouse	Greywacke, moderately strong.
M	TUZ, Tuapeka	Greywacke, moderately strong.
M	URZ, Urewera	Greywacke, deeply weathered, may be weak to moderately strong in top 30-40
M	WCZ, Waipu Caves	m.
W	WEL, Wellington	Triassic sandstone (greywacke), about 300 m thick over granite.
		Jurassic greywacke (siltstone), slightly weathered.
M-V	WHZ, Wether Hill Road	Small outcrop of ice-scraped granite, strong, in valley floor, part of the granite
M	WLZ, Whitehall	that forms the hills on the west of the Alpine fault in this area. It is next to a
V	WVZ, Waitaha Valley	huge zone of mylonite (fault breccia) associated with the Alpine Fault.

Notes: *1. Ground Classification*

V *rock outcrop, very strong rock*

M *rock outcrop, moderately strong rock*

W *rock outcrop, weak rock*

A1.3: Seismograph recording sites - TVZ Temporary Network.

Site class[1]	Site Code and Name	Subsurface Geology
M	ASHV, Ash Pit Road	Site on rock at foot of steep slope. Rangitaiki Ignimbrite in scarp above. Moderately strong rock.
W	DKRV, Dunkirk Road	On rock, on lower part of a steep slope near a stream. Ohakuri Group, water-laid pumice tuffs and breccias, sandstone and siltstone. Site close to Ngakuru Fault. Weak to very weak rock
W	EPAV, East Paeroa	Gentle hill slope. Close to contact between Paeroa Ignimbrite, Huka Group pumice breccia and tuff, and terrace or fan deposits. Weak rock.
M	ERQV, Earthquake Flat Rd	South flank of Tumunui Hill above Whirinaki Stream. Haparangi Rhyolite (1). Moderately strong rock.
M	ERRV, Earle Road Rocks	Talus covered slope at west edge of Rangitaiki Ignimbrite sheet. Site on rock outcrop, moderately strong.
M-W	GULV, Gully Road	In a gully 300 m from a quarry. Rotoiti Breccia? Reputed to be poorly compacted, but apparently moderately strong rock at site.
M	GV2V, Gavin Rd #2	In a gully. Rangitaiki Ignimbrite. Moderately strong rock.
W-M	HRXV, Hossock Rd Extn	On a small hill. Haparangi Rhyolite (2) on top of Paeroa Ignimbrite. Weak to moderately strong rock?
Soil	KPSV, Kapenga Swamp	In a small lobe of the swamp. Site on loose/soft soil, > 3 m deep, above Earthquake Flat Breccia.
M	OHPV, Ohinepanea	In disused quarry. Urewera Greywacke, fractured, close to extension of active fault trace. Moderately strong rock.
Soil	OKAV, Okareka	Close to edge of dome of Haparangi Rhyolite (1) (moderately strong rock). Site on soft soil (ash etc) > 3 m thick.
W-M	OKTV, Lake Okataina	Close to base of 40-50 m cliff in Haparangi Rhyolite (2). Moderately weak rock.
M	PKUV, Pukekahu	Site on rock at edge of small (~1km diameter) domed outcrop of Haparangi Rhyolite (1), moderately strong. Dome surrounded by low, marginally swampy ground. NB: Seismic response of dome very uncertain.
Soil	TAOV, Tarawera Outlet	Left bank of river close to lake outlet, gentle slope 20 m above lake. Haparangi Rhyolite (2), but thick talus blanketing slope. Site on soft to firm soil > 3 m deep.
W-soil	TEAV, Te Ana	Low, flat ground beside north arm of Lake Ohakuri. Taupo Pumice Alluvium overlying Huka Group lake sediments. Site on ignimbrite (boulder?).
Soil	WNUV, Wharenui	Beside stream below rim of Rotorua caldera. Site on soil > 3 m thick above Mamaku Ignimbrite (poorly welded, weak rock). Head of a stream. Haparangi Rhyolite (1), moderately strong rock, but overlain by soil etc., > 3 m deep.
Soil	WRAV, Wairua	On Waiotapu Valley Rd, undulating land. Site on soft/loose soil > 3 m thick above Huka Group – sandstone/ siltstone/pumice breccia.
Soil	WTPV, Waiotapu	Low saddle between heads of two streams. Ohakuri Group, water-laid pumice tuffs, breccias and sandstones and siltstones. Soil present at site but sensor reportedly on ignimbrite.
W	WVRV, Whirinaki	

Notes: *1. Ground Classification*

V	*rock outcrop, very strong rock*
M	*rock outcrop, moderately strong rock*
W	*rock outcrop, weak rock, plus class AV from Zhao et al. [30]*
soil	*soil layer > 3 m thick*